Supplementary Information

Reentrant DNA shells tune polyphosphate condensate size

Ravi Chawla[1,2,*], Jenna K. A. Tom[1,*], Tumara Boyd[1], Nicholas Tu[1], Tanxi Bai[1], Danielle A. Grotjahn[1], Donghyun Park[1], Ashok A. Deniz[1,#], Lisa R. Racki[1,#]

[1]Department of Integrative Structural and Computational Biology, The Scripps Research Institute, La Jolla, California, USA
[2]Current Address: Chakra Techworks Inc., 10918 Technology Place, San Diego, California, USA
*Equal contribution
[#]Corresponding authors: lracki@scripps.edu, deniz@scripps.edu

Supplementary Methods

Supplementary Table 1

Primer Name	Primer Sequence (5' to 3')
NTPR91 "PA14_lecAPro_(PlecA)_Fwd"	TTCAGCCGACTTCTGCGTTCCTT
NTPR92 "PA14_lecAPro_(PlecA)_Rev"	GATTGATCTCCGATATATGAATT
NTPR101 "ATTO488-5'_PA14_lecAPro_Fwd"	TTCAGCCGACTTCTGCGTTCCTT
NTPR102 "ATTO488-5'_PA14_lecAPro_Rev"	GATTGATCTCCGATATATGAATT

Characterization of the supercoiled fraction of DNA samples by native agarose electrophoresis

Sample preparation & Gel Processing

To identify and approximate the supercoiled fraction of our plasmid DNA samples, we prepared linearized controls as mobility references, which were DNA samples digested by restriction enzymes with unique cutting sites (see Supplementary Table 2 below for details) in 1x rCutsmart Buffer (NEB B6004S) at 37°C for 1 hour. For pUC19, we compared uncut to both linearized plasmid, and nicked DNA by using the site-specific nicking enzyme Nt.BspQI, which has a single recognition site within pUC19 to relax the DNA (Supplementary Fig.24).

For each DNA sample and its corresponding linearized control, 100ng of DNA was subjected to 0.5% or 1% agarose gel in 1xTAE (40 mM Tris, 20 mM acetic acid, 1 mM ethylenediaminetetraacetic acid) with no stain. The gels were post-stained with SYBR Gold (ThermoFisher Scientific S11494, 1:4000 dilution in 1x TAE) for 20 min and washed with MilliQ water three times before imaging with GelDoc Go Imaging System using the UV/Stain-Free Sample Tray (Bio-rad). SYBR Gold labeling is less sensitive to supercoiling state than other DNA dyes, and exhibits a linear relationship between DNA amount and fluorescence intensity[1,2]. For reference to other commonly-used DNA dyes, we compare a quantification of pUC19 using SYBR Gold to one using Ethidium Bromide, as well as the stain we used in our initial purification stages, APEX™ Safe (APExBio A8743) (Supplementary Fig. 24). Signal intensity of the supercoiled state band (determined based on its position and disappearance when linearized by restriction digestion, Supplementary Table 2) was used to assess the percentage of supercoiled DNA relative to other bands. Gel results are shown in Supplementary Figs. 23-26.

Supplementary Table 2

No.	Sample	Plasmid ID	Restriction Enzyme
1	2.7 kb	pUC19	KpnI-HF
2	5 kb	pETM6	KpnI-HF
3	8 kb	pLREX122	EcoRV-HF
4	10 kb	pLREX185	EcoRI-HF
5	15 kb	pVG1	KpnI-HF
6	20 kb	pEMS1107	KpnI-HF
7	25 kb	pEBTet-SNAP-ALMS1	EcoRV-HF
8	30 kb	pLD1 translation factors	SpeI-HF
9	5 kb-GC44	pLL346	EcoRV-HF
10	5 kb-GC53	pLREX240	KpnI-HF
11	5 kb-GC61	pOPTO328	EcoRV-HF

To test the effect of YOYO-1, 100 ng DNA samples and their corresponding linearized controls were prepared in 1 μM YOYO-1 in 1x rCutSmart buffer with the addition of 50 mM HEPES,100 mM $MgCl^{2+}$, to more closely mimic the conditions used for our condensate experiments for 9 min before being subjected to 0.5% or 1% agarose gel electrophoresis. Gel results are shown in Supplementary Figs. 26-27.

Gel quantification of the supercoiled fraction of DNA samples

The gel images were analyzed using FIJI/ImageJ (version 1.54f) to estimate the fluorescent intensity of specific bands. A manual rolling-ball background subtraction was applied to better present the fluorescent intensity of the bands (Supplementary Fig. 24). The supercoiled fraction ratio was defined as the ratio between the fluorescent intensity of the supercoiled band and that of all bands.

Preparation and Size Quantification of Circular and Linear DNA comparison

Linearization of pUC19 and 15kb plasmids was performed using Eco53kI (NEB Catalog #R0116S). Next, commonly used phenol-chloroform extraction was employed for purification of DNA[4]. To account for and eliminate any processing-specific differences, circular pUC19 and 15kb DNA were subjected to similar phenol-chloroform extraction steps, serving as control samples. The circular and linear DNAs were then used for droplet experiments for microscopy and Cryo-ET experiments as noted previously in the manuscript. Size quantification was carried out as per size quantification protocols described previously. Four runs were collected with YOYO-1, while two were done in the absence of YOYO-1. Experiments without YOYO-1 are internally consistent with the two of the four done with YOYO-1, performed on the same day and indicated in Supplementary Fig.11 by the shared experiment number.

Plasmids

pETM6 was a gift from Mattheos Koffas (Addgene plasmid # 49795 ; http://n2t.net/addgene:49795 ; RRID:Addgene_49795)

pVG1 was a gift from Gerald Fink (Addgene plasmid # 111444 ; http://n2t.net/addgene:111444 ; RRID:Addgene_111444)

pEMS1107 was a gift from Elizabeth Simpson (Addgene plasmid # 29036 ; http://n2t.net/addgene:29036 ; RRID:Addgene_29036)

pEBTet-SNAP-ALMS1 was a gift from Kai Johnsson (Addgene plasmid # 136828 ; http://n2t.net/addgene:136828 ; RRID:Addgene_136828)

pLD1 translation factors was a gift from Anthony Forster (Addgene plasmid # 117760 ; http://n2t.net/addgene:117760 ; RRID:Addgene_117760)

pLL346 and **pOPTO328** were gifts from Keren Lasker

pLREX122 was created by Gibson assembly (NEB Gibson Assembly Master Mix, E2611) using pJM220[5] cut with KpnI as the vector backbone and a 399bp PCR product using pMQ72[6] as template, amplified with primers LRPR934 and LRPR935. The correct insert was confirmed by Sanger sequencing.
LRPR934:
GAATTCCTCGAGAAGCTTGGGCCCGGTACCTCGCGAATCAGAACGCAGAAGCGGTCTG
LRPR935:
GGAACTAGATTTCACTTATCTGGTTGGCCTGCAAGGCCTTATGCCTGGCAGTTTATGG

pLREX185 was created by Gibson assembly (NEB Gibson Assembly Master Mix, E2611) using pMQ30[6] cut with HindIII and KpnI as the vector backbone and two PCR fragments: (1) 1126bp using *P. aeruginosa* PAO1 genomic DNA as template and primers PCPR1 and PCPR2, and (2) 2008 bp using *P. aeruginosa* PAO1 genomic DNA as template and primers PCPR3 and PCPR4. The correct insert was confirmed by Sanger sequencing.
PCPR1:
CCAGTCACGACGTTGTAAAACGACGGCCAGTGCCAAGCTTATGCCTAACCTCACCCTTGC
PCPR2:
AGATTCATGAAAGCTCAAAAAGGTTGTGATAACTAAGGTG
PCPR3:
TCACCTTAGTTATCACAACCTTTTTGAGCTTTCATGAATC
PCPR4:
GAAACAGCTATGACCATGATTACGAATTCGAGCTCGGTACCTTAATCCTTGGTCACGCGG

pLREX240 [5.5kb-GC53] was created by Gibson assembly (NEB Gibson Assembly Master Mix, E2611) using plasmid pETM6[7], linearized using XbaI and NdeI, was used as the vector backbone. A linear 414bp DNA fragment (sequence below) was assembled into the linearized

plasmid using the NEB Gibson Assembly Master Mix (E2611) Assembly protocol. The master mix was cleaned up using DNA cleanup Kit (NEB, catalog# T1030S) and transformed into electrocompetent DH5 alpha cells using electroporation. Whole plasmid sequencing was used to identify successful candidates for assembly of ~5.5kb plasmid.

Sequence of 414 bp linear insert:

ggggaattgtgagcggataacaattcccctctagaATGGTCAGCAAGGGGGAGGAGGACAATATGGCCTCGCTGCCC
GCGACCCACGAACTGCACATCTTCGGGTCCATCAACGGGGTCGACTTTGATATGGTGGGCCAAGGG
ACCGGCAATCCCAACGACGGCTATGAGGAACTGAATCTCAAGTCGACGAAGGGGGACCTCCAGTTTA
GCCCGTGGATCCTCGTGCCCCATATCGGCTATGGCTTCCACCAATATCTGCCGTATCCGGATGGGATG
AGCCCGTTTCAGGCCGCCATGGTGGACGGGAGCGGGTATCAGGTCCACCGGACGATGCAGTTTGAA
GATGGCGCGAGCCTGACGGTCAATTATCGTTATACGcatatggcagatctcaattggatatcggccggcc

Plasmid preparation for GC content comparison

Three 5.5 kb plasmids (pLL346 (44%GC), pLR240 (53%GC) and pOPTO328 (61%GC)) were isolated using Midi-prep. Plasmids pLL346 and pOPTO328 were a gift from Keren Lasker's laboratory. Concatemers were observed in plasmids other than pLL346. To eliminate the confounding effects of concatemers and standardize the plasmid state, an electro-elution setup was used to isolate and purify the three circular plasmids. Electro-Eluter (Bio-Rad, Model 422) was used per the specification in the manufacturer's instruction manual. Briefly, ~30 µg of each plasmid was run on separate 1% agarose gels (stain-free). Bands corresponding to 5.5 kb plasmids were identified and isolated using a combination of a 1 kb Plus ladder (NEB, Catalog# N3200S) and sacrificial lanes in the agarose gel post-stained with APEX™ Safe stain. Excised stain-free gel was used for DNA elution. Eluted DNA was then buffer-exchanged into deionized water using manufacturer recommended filtration protocol(Millipore, 100kDa MWCO, UFC510024).

Quantification of Relaxation Time

Sample Preparation of DNA-polyP-Mg^{2+} condensates

Preparation of condensates was done as described previously for DNA concentration experiments. In brief, DNA, buffer, and P700 (composed of roughly 10% AF647-labeled P700) were premixed, followed by droplet induction with equal volume Mg^{2+} such that final concentrations were: polyP = 1mg/mL, DNA = 10ng/µL (or 100ng/µL for 10X pUC19), HEPES = 50mM, and Mg^{2+} = 100mM. Immediately after addition of Mg^{2+}, the solution was transferred to a Tween coated Lab-Tek slide as described in the Methods section. For samples analyzed in this data set, no YOYO-1 was added.

Fusion event imaging & processing

For each DNA condition, three experimental runs were conducted. Each experiment sampled three time lapse series, each in a different area, spanning two minutes (roughly started at 7.5, 10, and 12.5 minutes after droplet formation). Images were collected using Zeiss 780 confocal

microscope with an excitation at 633 nm laser set at 3% power. Pixel dwell time was set at 1.27μs, and images were conducted with no delay, resulting in an interval of 392.51ms between frames. Fusion events of two droplets were manually identified and cropped in FIJI to roughly center and isolate the fusion event.

Fusion event image analysis & fitting

Using custom Python code, these images were thresholded using Otsu thresholding, converted to a binary image, and cleaned using skimage modules. Regions were labeled based on connectivity of the cleaned image, and subsequently fit with ellipses, recording the area, major axis, and minor axis per frame. The frame where fusion initiation begins was identified as the first point that met three conditions after exclusion of segmentation blips (defined as a point which has a change with a magnitude of >0.7 in aspect ratio consecutively in opposite directions): a) the next three points from that point decrease, b) the first decrease has to be at least 12%, the second 8%, and the third 4% after correcting for the minimum baseline at 1, and c) the starting point aspect ratio must be greater than 1.4. The first two above conditions detect consecutive decreases larger than noise for this particular dataset, while the last condition prevents small changes on the baseline from being detected. Time zero corresponds to the identified frame with subsequent frames offset by the image scan time, 0.39251s.

Aspect ratio was calculated by dividing the major axis by the minor axis, and points from fusion initiation on were fit using the standard equation:

$$A = 1 + (A_0 - 1)e^{-\frac{t}{\tau}}, \qquad (1)$$

where A = the aspect ratio at time t and A_0 and τ are fitting parameters corresponding to the aspect ratio at time 0 and relaxation time constant respectively. Tau for each event was then plotted as a function of half the major axis converted to microns at time = 0 to show the rough relaxation constant for each event observed as a function of length scale.

Fusion events were removed if i) the fusion event had fewer than 10 segmented frames, ii) no zero point or fusion initiation was able to be identified based on the above conditions, or iii) if segmentation translated to difficulty in isolating and identifying the droplet pair (ie: if a third droplet was segmented into the region and prevented the curve fit from identifying the proper zero or significantly pulling the fit from the curve). In total, 28 fusion events for the no DNA condition were collected, along with 48 pUC19 (1x), 17 (15kb), and 20 pUC19 (10x) from the three experiments (or 9 two minute movies). The pUC19 fusion events were further analyzed and fit to a linear curve. No YOYO-1 was added.

Whole Droplet FRAP

Whole Droplet FRAP was conducted using the same protocol as partial droplet FRAP, noted in the Materials & Methods main text with adaptations described here.

Slide preparation for whole droplet FRAP

To observe recovery of a whole droplet bleaching, we needed condensates to meet the following conditions: the droplet observed a) cannot undergo fusion on the time scale of our

measurement, b) has to remain relatively stable in its position, and c) is not so large that recovery is near the limits of detections. Because no DNA and pUC19 (1X) droplets grow relatively quickly to large sizes before settling on the coverglass, we changed our approach to settle the same volume of droplet solution on a larger surface area to suppress fusion and growth.

A surface of 22mm x 22mm High Precision coverslips (Azer Scientific, ES0107052, #1.5H) were Tween coated by incubating 240µL of 10% Tween solution on the coverglass for 35 minutes. Slips were washed with MilliQ water 6-7 times and dried by blow drying with air. Coverglass was left out to air dry for at least another hour before use.

To a 3”x1”x1” microscope slide (VWR, 16004-430). Tween-coated coverslips were roughly centered on the slide, coated surface facing inward, with double-sided tape (Scotch 3M) separating the two glass layers on two sides to form a thin channel.

Sample preparation of polyP-Mg^{2+} condensates for whole droplet FRAP
Samples were prepared in the same way as whole droplet FRAP samples. Rather than addition to LabTek slides, samples were immediately pipetted into the channel from one end until full and sealed with nail polish on the remaining ends. Slides were inverted on falcon tube caps to allow for settling on the coverglass, and nail polish was allowed to dry for >8 minutes before transferring the slide to the microscope stage. FRAP imaging was conducted on samples from 20-120 minutes after droplet formation and sealing.

Whole droplet FRAP bleaching, post-processing, and analysis
The same bleaching protocol as described for partial droplet FRAP was applied to whole droplets approximate 3 µm in diameter. Following bleaching, images were collected in 2.5s intervals for 12 minutes with reflection autofocus being applied every 120 scans or roughly every 5 minutes.

Rather than aligning single droplets in StackReg, the 400x400px image frame acquired was cropped and aligned using StackReg ‘Translation’ transformation to account for xy slide drift provided non-analyzed droplets were stable enough on the coverglass. For cases where background droplets were highly mobile (pUC19), no registration and alignment was applied. Normalization and fitting was handled as described in the Main text. Data sets shown are truncated at 10.02 minutes.

Widefield Image Dynamic Range Adjustments

For polyP visualized with the 640 channel, the min and max were set to 1616 and 15601 respectively, while values of 904 and 23335 were used for DNA shells visualized with the 488 channel (Supplementary Figs. 13 & 18). In Supplementary Fig. 13, the brightfield image min was set to 4438 and the max at 34318. We also adjusted the dynamic range for the following SI figure panels: Supplementary Fig 1 (CH1(647nm): min = 2075, max = 5426; CH2(brightfield): min = 15124, max = 46823), Supplementary Figs. 2b, left (CH1(647nm): 4231) and right

(CH1(647nm): min = 3756, max = 14009, CH2(488nm): min = 4682, max), Supplementary Figure 11 (CH2: min = 3541, max= 6393), and 23b (P_{lecA}: min = 3808, max = 13219 (inset: min = 3967, max = 5395), pUC19+YOYO1: min = 3034, max = 5808). No other image intensity modifications were made.

PolyP300 AlexaFluor647 labeling and purification

PolyP300 was labeled and purified using the same protocol as used for polyP700 labeling, noted in Material & Methods in the main text, adapted from published methods[8,9], with the following final reagent concentrations: 7.5 mg/mL polyP300 (500 μM free ends), 200 mM EDAC, and 10 mM AlexaFluor647 cadaverine (20-fold excess), in 100 mM MOPS pH 8.0. The reaction conditions and excess dye removal steps were the same as for polyP700 labeling.

PolyP on gel electrophoresis

PolyP size distributions were resolved using gel electrophoresis using an established protocol[10]. In brief, 100-1000 nmol polyP suspended in loading buffer (1X TBE, 3% Ficoll 400, 0.02% bromophenol blue) were loaded to 5% acrylamide TBE gels (Bio-Rad, #4565013). Samples were run at 150 V for 22 min at 25°C. Gels were stained in destain buffer (25% methanol, 5% glycerol) with 0.05% toluidine blue for 10 min with rocking. Two ladders were used: O'RangeRuler 10 bp DNA Ladder (Thermo Sci., SM1313, shown in the Source Data File) and 100 bp DNA Ladder (NEB, N3231S). Gels were destained in destain buffer for 1 hr with rocking per wash and repeated for a total of three washes. Imaging was performed using white light on a GelDoc Go (Bio-Rad, # 12009077).

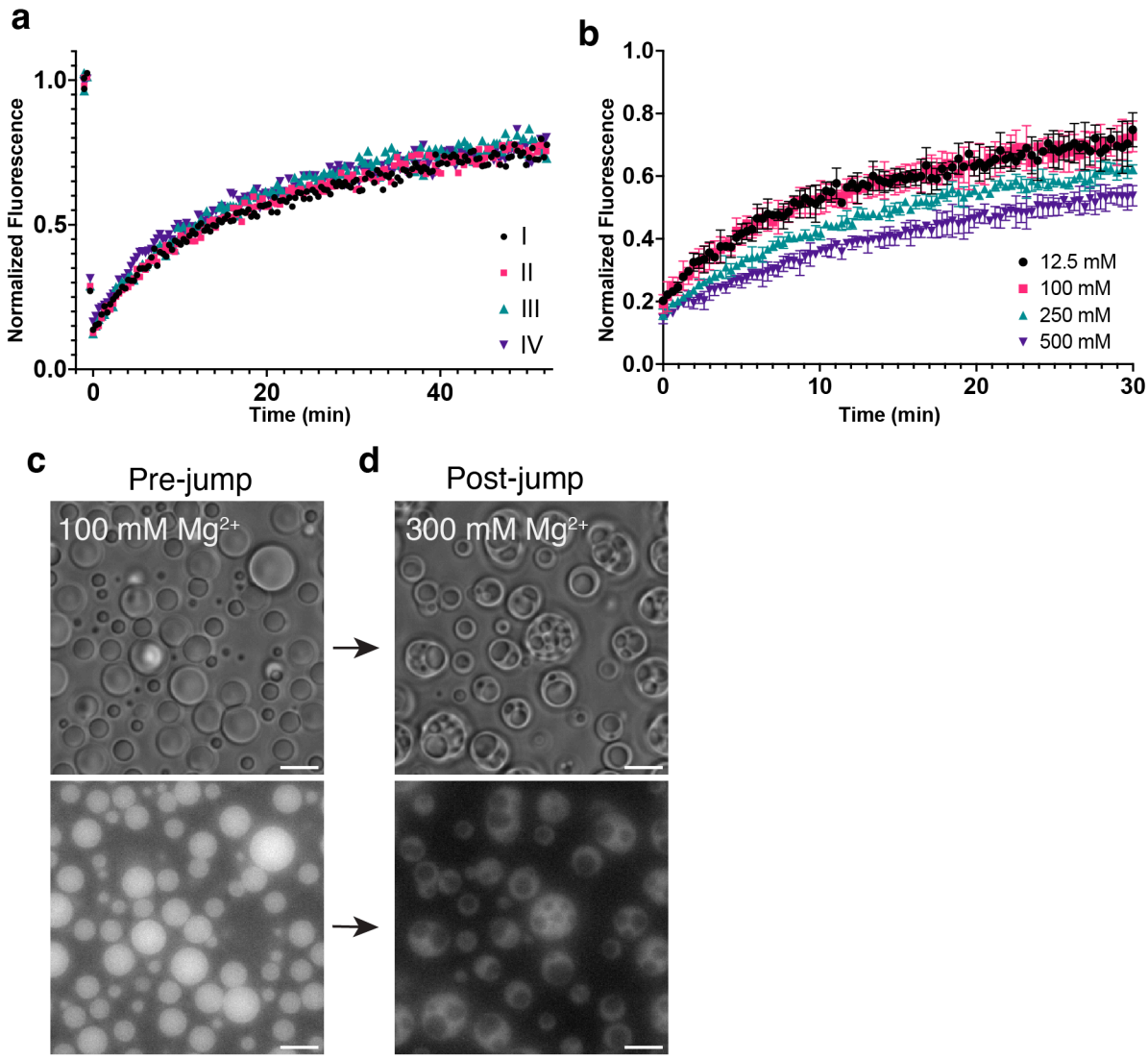

Supplementary Fig. 1. a) Overlay of individual FRAP experiments for polyP-Mg^{2+} condensates. Condensates were allowed to grow for 35-45 minutes after which a small circular region in the center of the condensate was bleached. Scans were taken every 20s for 52 minutes with autofocus z corrections being applied every 15 images (~5 min). New samples were prepared for each experiment. Each run takes place between 35-100min after droplet formation. The time zero on the graph is the scan immediately following the bleach. b) FRAP experiments of polyP-Mg^{2+} condensates at different Mg^{2+} concentrations. Points represent an average of 3-4 runs and error bars show the standard deviation (n=3: 12.5mM, 100mM, n=4: 250mM, 500mM). FRAP curves were collected for ~32 minutes, with new samples prepared for each experiment. c-d) PolyP-Mg^{2+} condensates form vacuoles upon addition of Mg^{2+} to preformed droplets. c) PolyP-Mg^{2+} condensates were formed (1 mg/mL polyP, 100mM $MgCl_2$, 50 mM HEPES pH 7.5, scale bar = 5μm) and allowed to fuse and grow for 10 min. d) Mg^{2+} concentration was subsequently brought to 300mM. Within a minute of $MgCl_2$ addition, vacuoles were observed. These vacuoles fused (Supplementary Movie 1) and were transient.

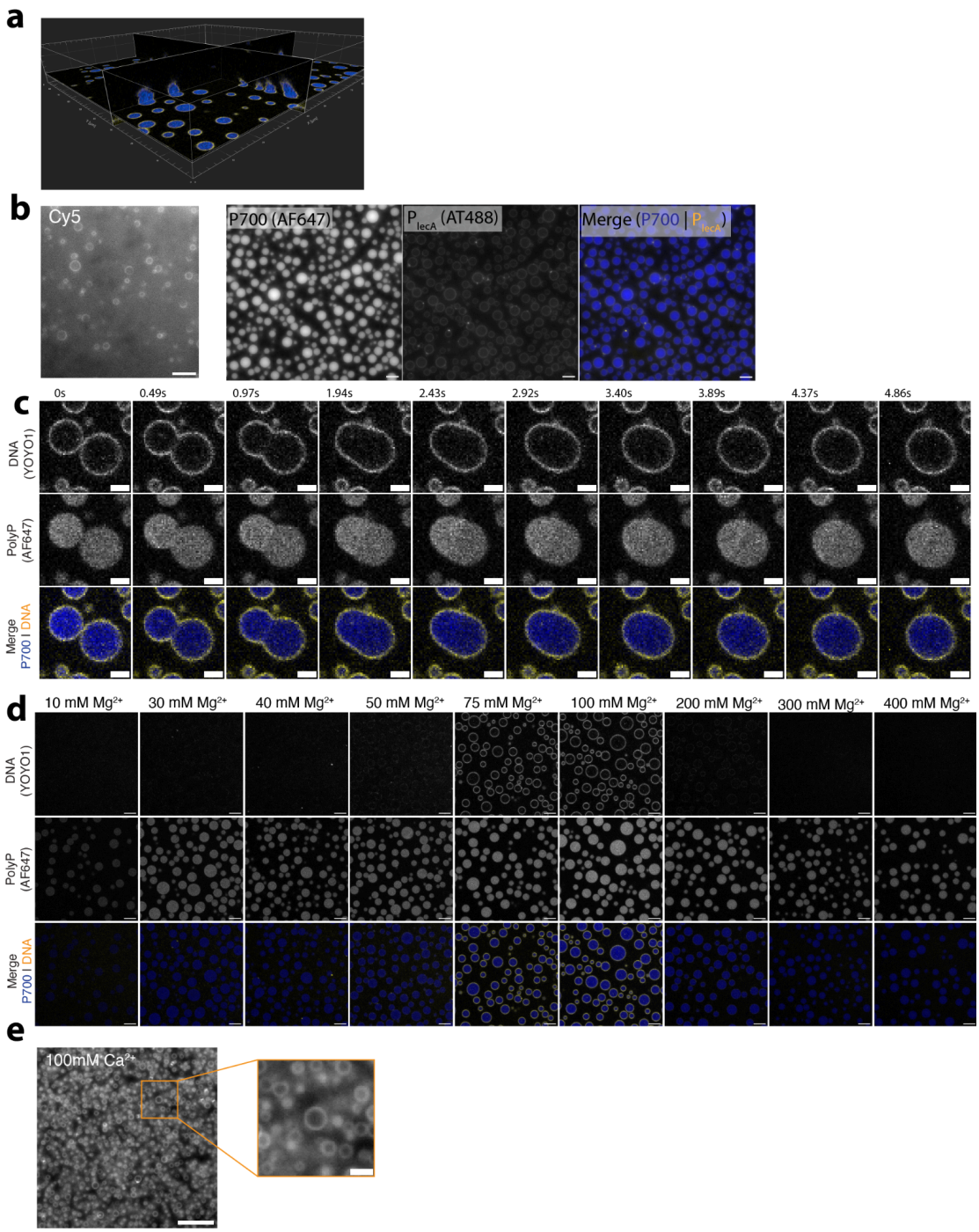

Supplementary Fig. 2. a) Imaris-rendered ortho slices of polyP-Mg^{2+}-pUC19 shelled condensates (1mg/mL polyP (10% P700-AF647, blue), 100mM Mg^{2+}, 10ng/μL pUC19 (1μM YOYO-1, yellow)). b) DNA shells visualized using two different covalently labeled DNA: 5' end-labeled Cy5 (left, [pUC19] = 5 μg/mL, scale bar = 10μm) and the 400bp PCR fragment, ATTO488-P_{lecA}, (right, [DNA] = 10μg/mL, scale bar = 5μm) c) Frame-by-frame visualization of P700-Mg^{2+}-pUC19 condensate fusion (scale bar = 2μm). d) DNA shells show reentrant behavior, appearing between 50mM and 200mM Mg^{2+} (scale bar = 5μm). e) P700 condensates also form in the presence of Ca^{2+} (1mg/mL polyP, 100 mM $CaCl_2$, scale bar (main) = 10μm, scale bar (inset) = 2μm).

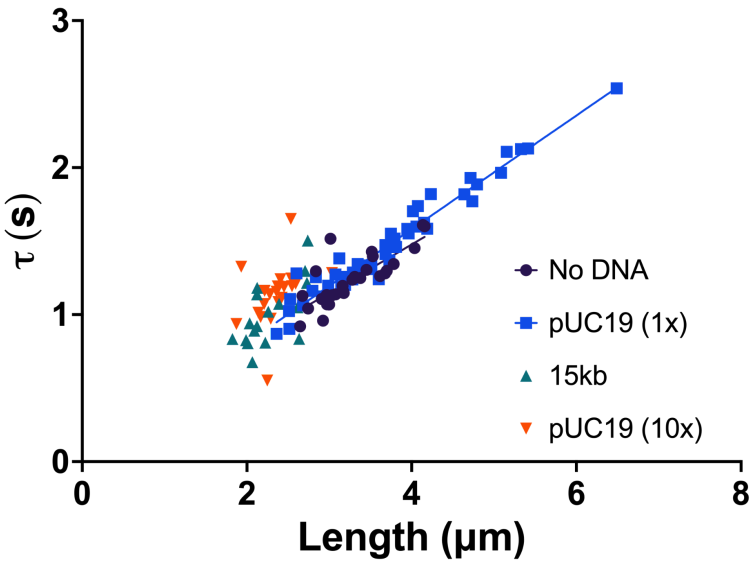

Supplementary Fig. 3. Passive fusion relaxation time as a function of approximate average droplet size for polyP-Mg^{2+} condensates with No DNA (Navy, circle, n=28), 10 ng/μL pUC19 (Blue, square, n = 48), 10 ng/μL 15kb (green, triangle, n = 17), and 100 ng/μL pUC19 (orange, inverted triangle, n =20). The average diameter (μm) of the droplet pair was estimated by dividing the length of the major axis in the first frame of fusion initiation by two. We believe this generally shows that the time scale of relaxation for condensates is similar across our DNA conditions, and occurs over a few seconds which is relatively fast (95% decay ~3τ)

Supplementary Note 1: Typically, for a Newtonian fluid, the relaxation time constant is proportional to the length scale on which deformation occurs as well as the inverse capillary velocity or the ratio of viscosity and surface tension. As such, for a Newtonian fluid in absence of other resistive forces, this value can be estimated using the slope of a length vs relaxation time graph as we have shown above. For reference, we did so for our polyP-Mg^{2+} condensates incubated with no DNA and 1X pUC19. The resultant slope with no DNA was 0.33 ± 0.05 using standard error and 0.39 ± 0.01 with 1X pUC19 (95% confidence intervals: 0.23 to 0.43 and 0.36 to 0.41 for no DNA and 1X pUC19 respectively)*. Using this simplified model and assuming that the internal viscosity of polyP-Mg^{2+} condensates is similar for DNA and no DNA cases, this could imply that the surface tension is slightly reduced in the DNA case.

***However, we believe there are several caveats in interpreting these values including:**

1. **Newtonian fluid & applicability of model.** Without further material state analysis, it is not apparent that this particular system is a Newtonian fluid. Increasingly, work in the field demonstrates the potential for many biological condensates to have viscoelastic properties. Thus, in absence of more precise material state quantification, we cannot say for certain whether this particular model, which assumes a Newtonian fluid, is appropriate[11–13].
2. **Interaction with surface.** Passive droplet fusion as opposed to optical tweezer based studies has several weaknesses, including that imaging typically takes place with droplets on the coverglass surface. Even though our system shows minimal wetting, friction or other resistive forces from condensate/surface interactions may increase the relaxation time constant. This is especially relevant if we were comparing across different DNA conditions given the potential for different surface coverage of condensates and thus different interactions with the same surface.
3. **Estimation of condensate size by confocal microscopy.** We used confocal microscopy as opposed to the widefield microscopy we used for our size quantification experiments. This was a choice made to get a higher signal-to-noise of our fluorophore and to avoid some of the haloing we observe in widefield with larger droplets observed at extended times. However, this means that we are observing a narrower cross-section slice which has the potential to decrease the accuracy of condensate size depending on the plane of analysis (ie: droplets might appear smaller if the plane is not centered perfectly in the z dimension). For samples with a wider size distribution per FoV, this confounding factor should have a stronger effect.

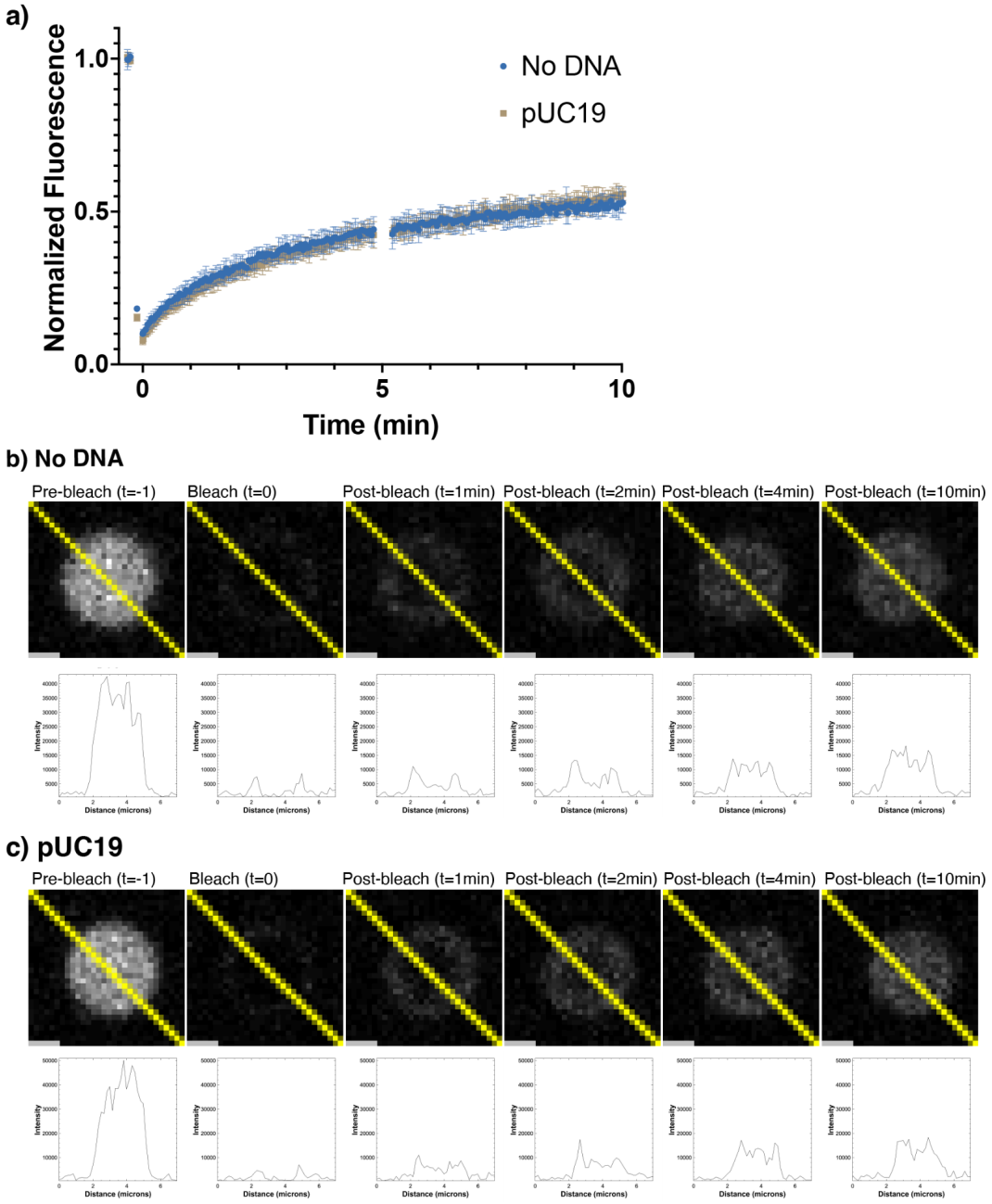

Supplementary Fig. 4. Whole droplet FRAP of polyP-Mg^{2+} condensates in the presence and absence of DNA (1 mg/mL polyP [~10% P700-AF647], 100mM $MgCl_2$, 50 mM HEPES pH 7.5, ±10ng/µL pUC19). a) Recovery of polyP-AF647 in polyP-Mg^{2+} condensates over 10 minutes in the presence (blue, n = 4) and absence (yellow, n = 3) of 10ng/µL pUC19. Condensates approximately 3µm in diameter and containing ~10% AF647-labeled polyP were bleached. Points and error bars represent the mean and standard deviation respectively of replicates in a set. b-c) Representative images and line scans showing radial recovery for bleached condensates in the absence (b) and presence (c) of DNA (scale bar = 1µm, overlay (yellow) = line scan).

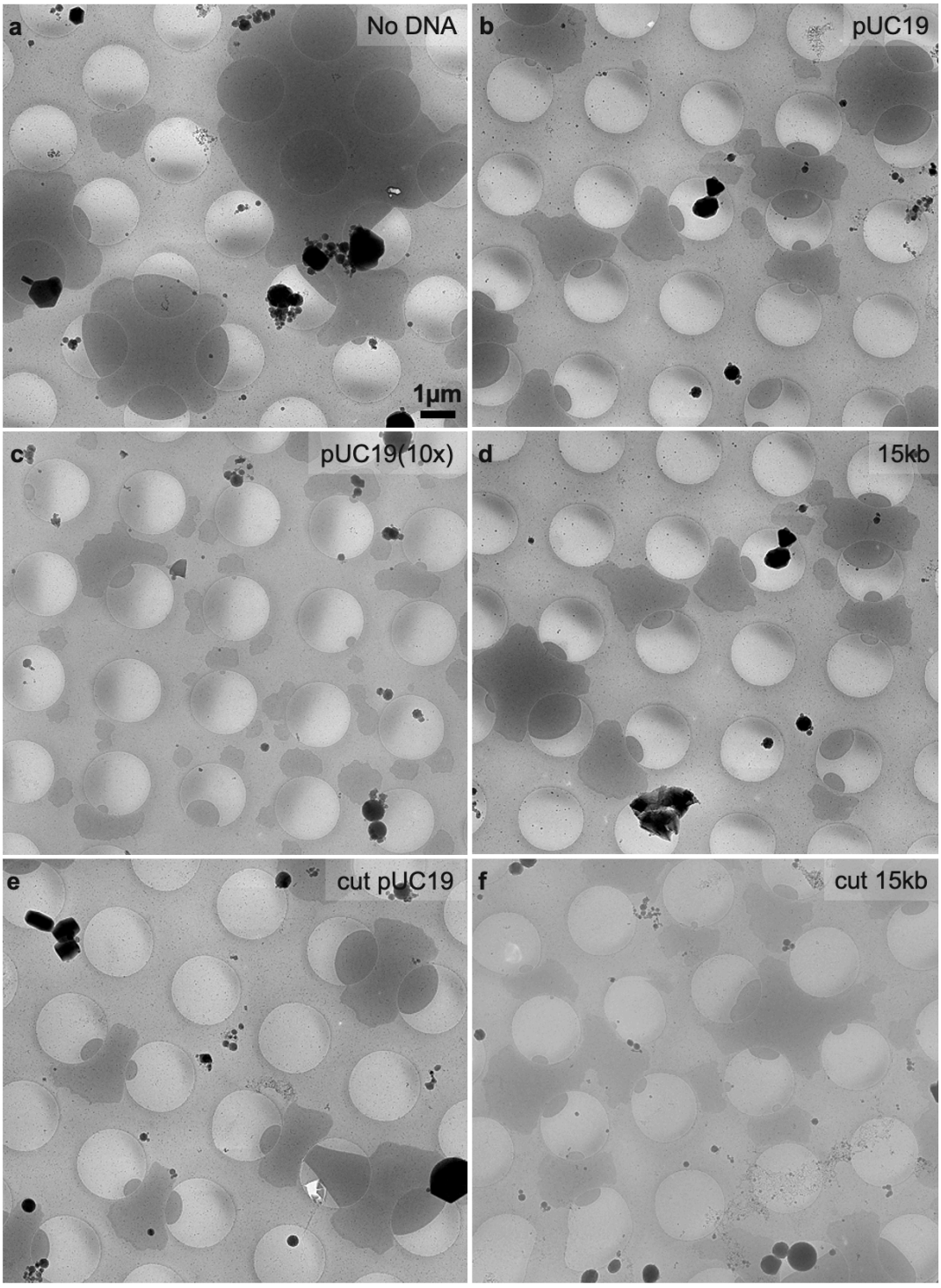

Supplementary Fig. 5. Low-magnification cryo-electron microscopy (cryo-EM) images of polyP condensates with various types of DNA on cryo-EM grids: (a) polyP only, (b) polyP + circular pUC19, (c) polyP + circular pUC19 (10x), (d) polyP + circular 15kb , (e) polyP + linear pUC19, and (f) polyP + linear 15kb.

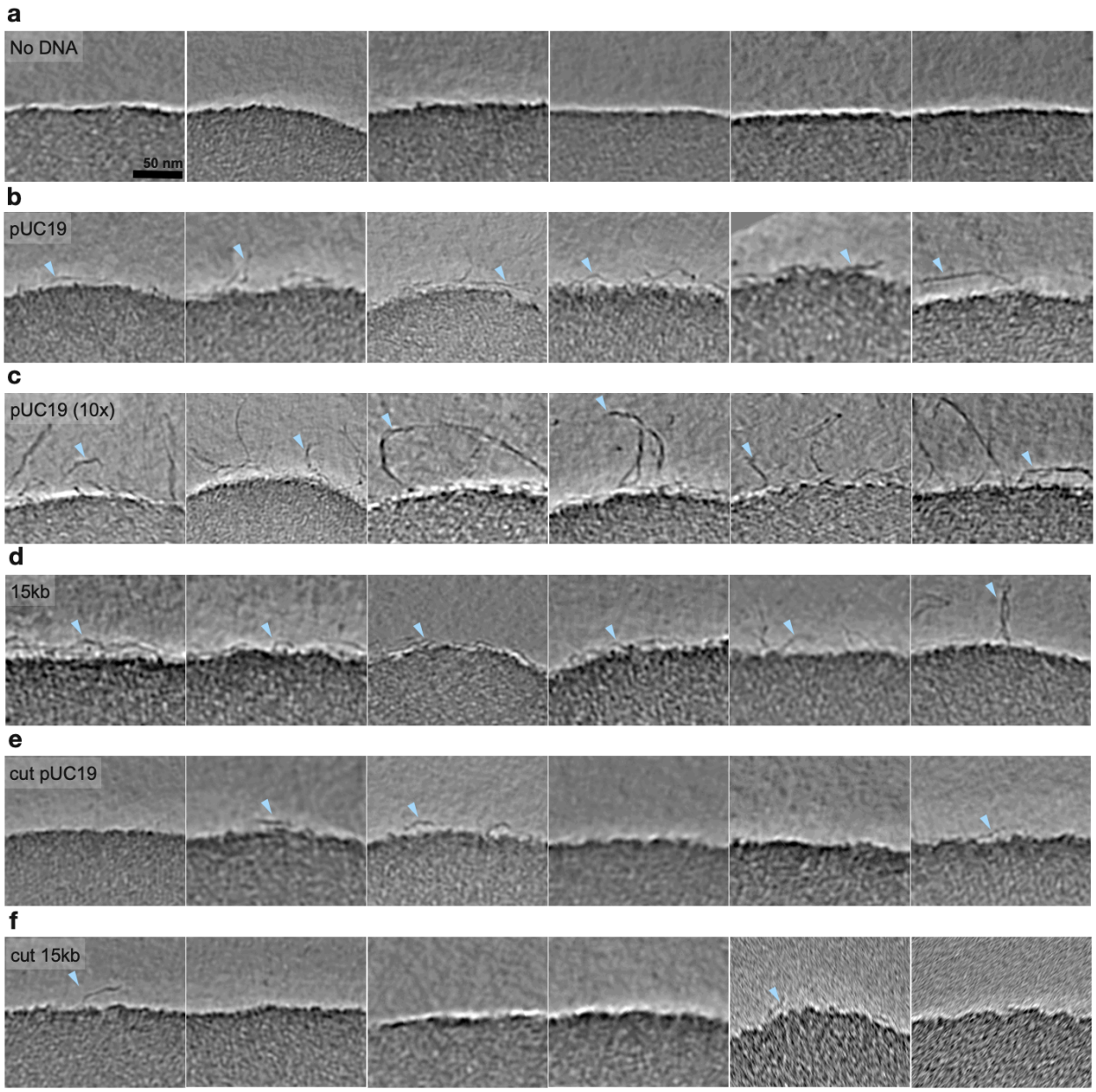

Supplementary Fig. 6. Gallery of snapshots showing the surface of polyP condensates incubated with different types of DNA: (a) No DNA, (b) pUC19 (10ng/μL), (c) pUC19 (10x) (100ng/μL), (d) 15kb (10ng/μL), (e) linearized pUC19 (10ng/μL), (f) linearized 15kb (10ng/μL) [1mg/mL polyP, 100mM Mg^{2+}, 50mM HEPES, pH 7.5; scale bar = 50 nm]. Cyan arrows highlight DNA that sticks out of the surface.

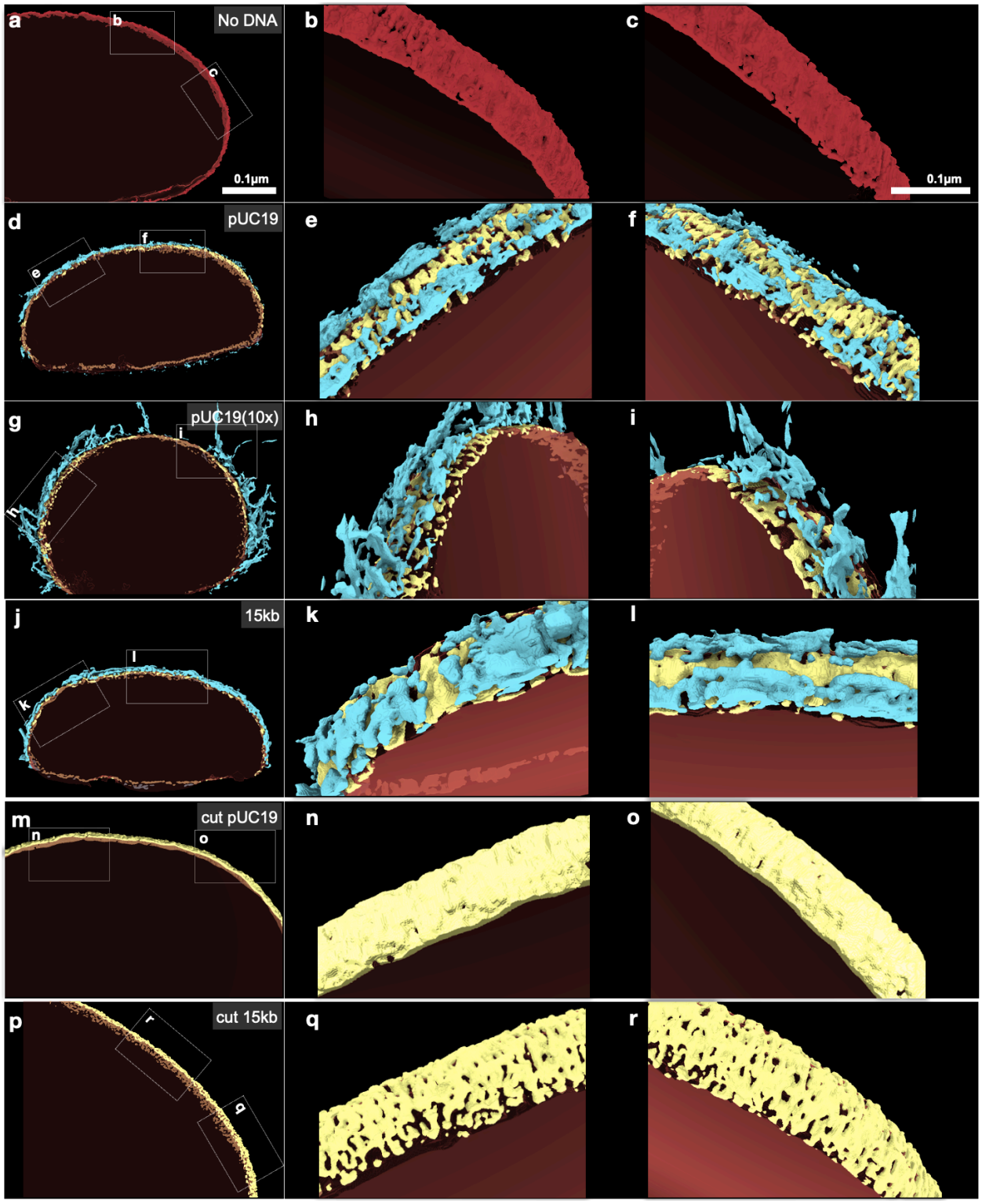

Supplementary Fig. 7. Surface texture of polyP-Mg^{2+} condensates interacting with different types of DNAs: (a-r) 3-dimensional renderings of tomograms shown in Figure 3 in both top-down views (a, d, g, j, m, p) and surface views (b-c, e-f, h-i, k-l, n-o, q-r). PolyP condensate edges are shown in red, DNA filaments are in cyan, and the ambiguous polyP-Mg^{2+} dense edge and DNA surface is in yellow (scale bar = 100 nm).

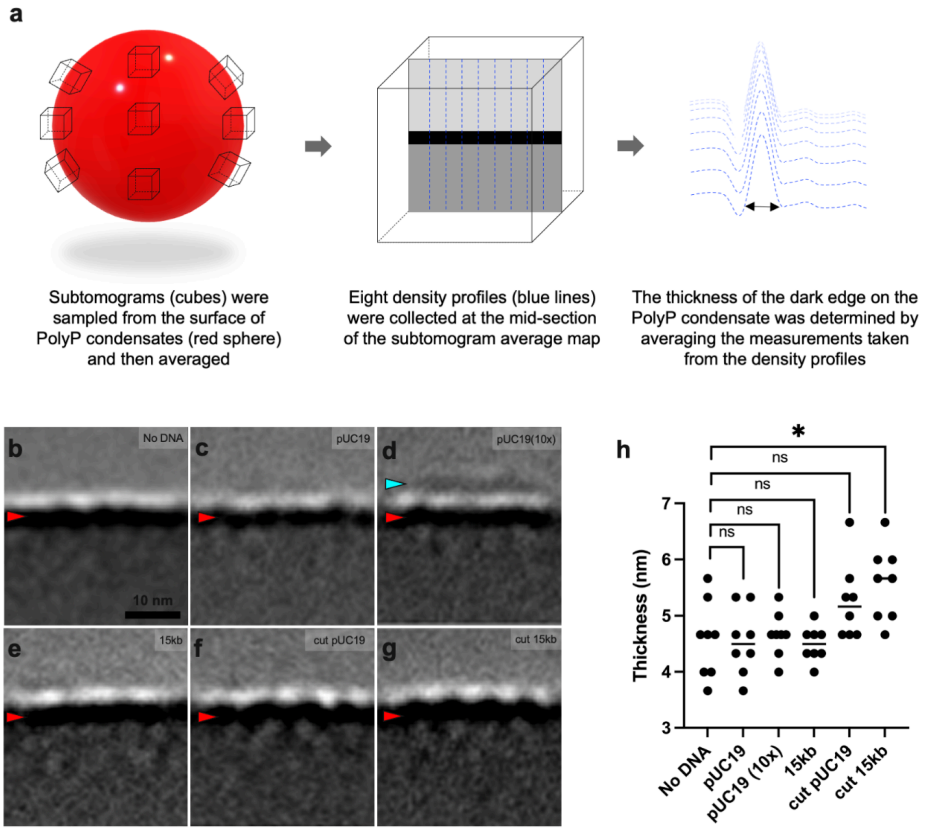

Supplementary Fig. 8. (a) A cartoon model depicting the subtomogram sampling process and the thickness measurement. (b-g) Subtomogram averages of the surface of polyP condensates incubated with different types of DNA. Red arrows indicate the dense edges of condensates, and the cyan arrow in panel e indicates extra density found only in this experimental condition. (h) Comparison of condensate edge thickness. The thickness of the dark edges was measured as described in Panel a. The measured thickness values for the different samples are as follows: (b) 4.6±0.7 nm, (c) 4.5±0.6 nm, (d) 4.7±0.4 nm, (e) 4.5±0.3 nm, (f) 5.2±0.7 nm , (g) 5.6 ± 0.7 nm (scale bar = 10nm). Statistical significance was calculated using one-way ANOVA with the Tukey HSD multiple comparison test.

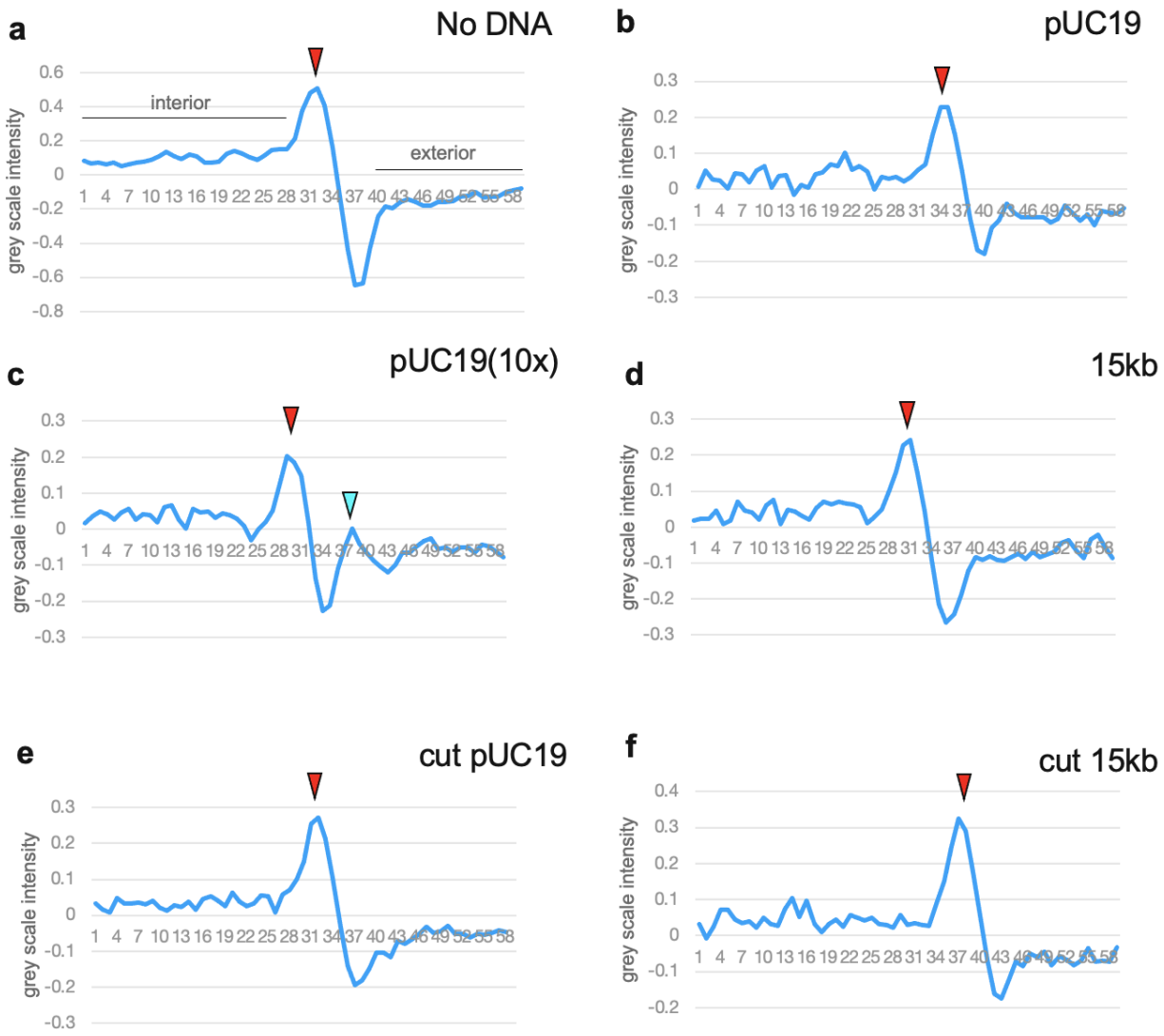

Supplementary Fig. 9. (a-f) Representative density profiles. The x-y plane density profile is drawn perpendicular to the direction of the dense edge. The X-axis represents the vertical span of pixels (6.65Å/pixel), extending from the bottom to the top of the average map. The Y-axis represents grayscale values ranging from -1 (white) to +1 (black). Red arrows indicate the dense edges of condensates, and the cyan arrow in panel d indicates extra density found only in this experimental condition.

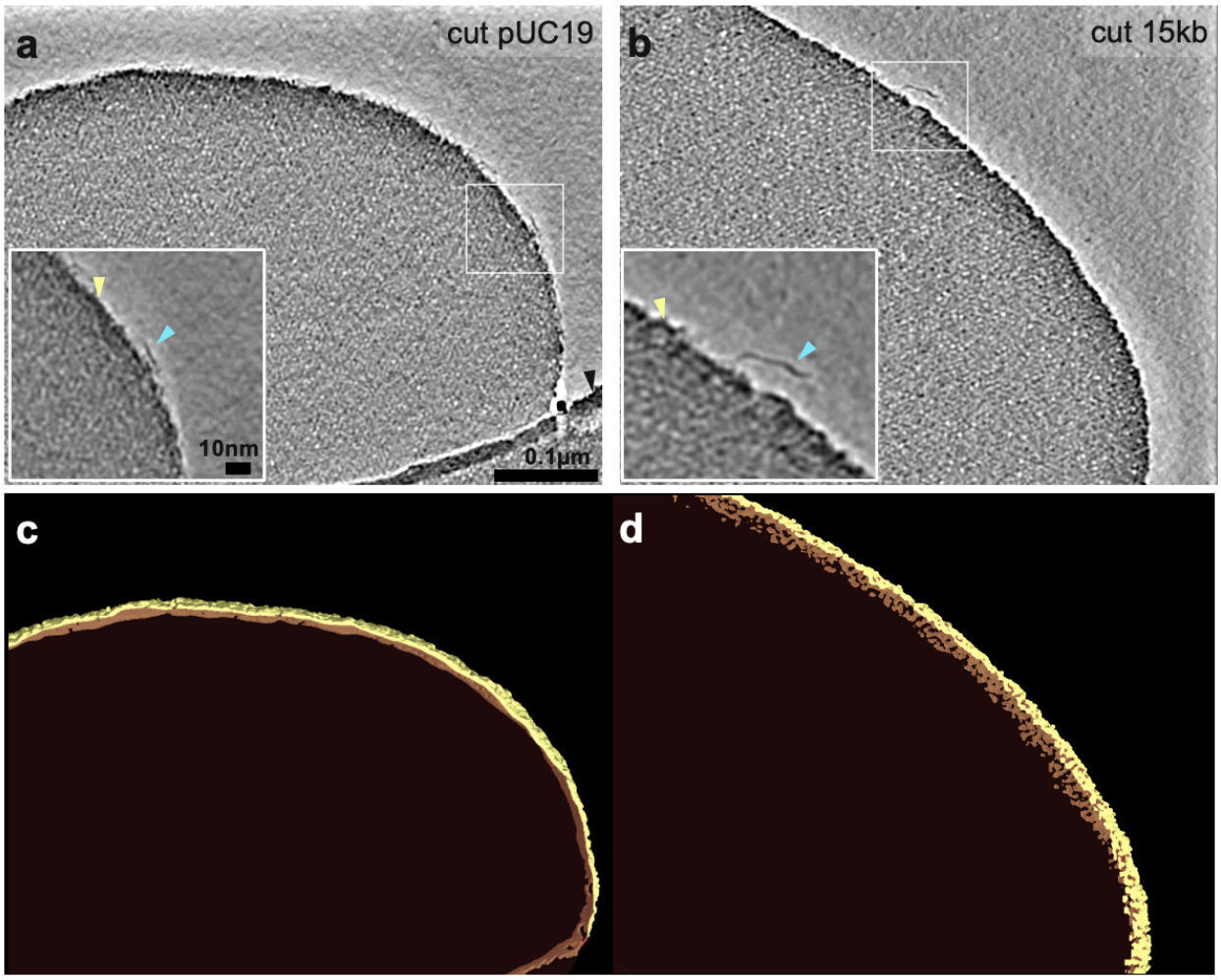

Supplementary Fig. 10. Cryo-electron tomography of linearized pUC19 and 15kb DNA. (a-b) Representative tomographic slices of polyP condensates incubated with linearized (a) pUC19 and (b) 15kb DNA. Cyan arrows highlight DNA, yellow arrows highlight the dense edge+DNA surface, and the black arrow highlights the edge of the carbon hole (scale bar = 100 nm, inset scale bar = 10nm). (c-d) 3-dimensional renderings of tomograms shown in panels a and b, respectively. The dense edge of polyP condensate is shown in red, the dense edge+DNA are shown in yellow.

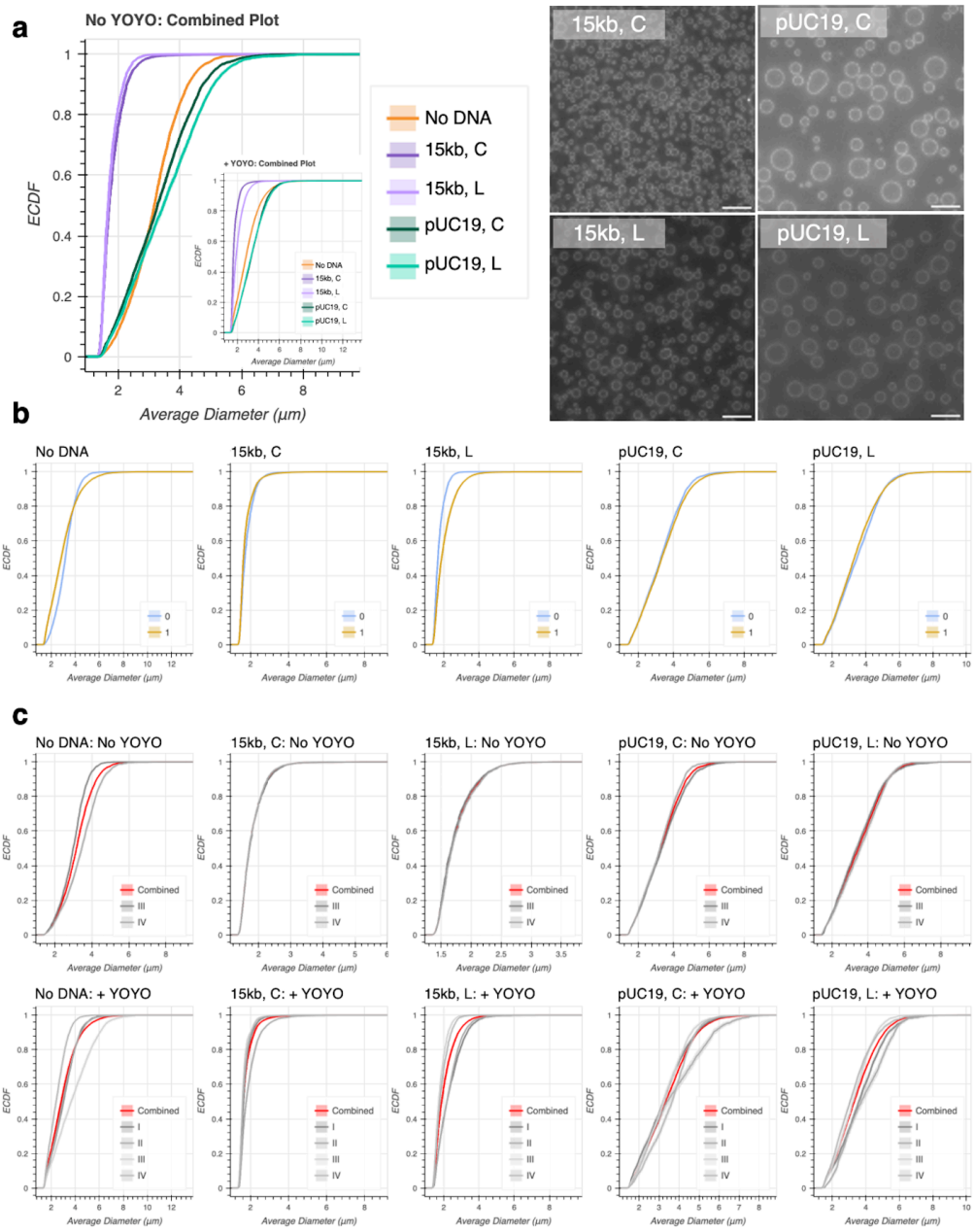

Supplementary Fig. 11. Size quantification comparison using circular and linear pUC19 and 15kb plasmids. (a) *left:* The combined ECDF for polyP-Mg^{2+} condensates in the presence and absence of linear and circular pUC19 and 15kb plasmids. The combined experiments with no YOYO-1 (n = 2) are shown in the main graph and inset with the corresponding plot conducted under conditions with YOYO-1 (n = 4) . *right*, Representative images from the YOYO-1 channel to demonstrate that shell formation is still observed with linear and circular DNA (scale bar = 10μm, n = 1). (b) direct comparison of the combined ECDFs for different DNA conditions in **a** with YOYO-1 (orange, 1μM) and without (blue, 0μM). (c) ECDF curves showing cumulative size distributions at 10min for varied DNA conditions for individual experiments (grey) with the corresponding combined distribution curve used in overlaid for reference (red). Shaded regions behind the solid line represent 95% confidence intervals calculated through Iqplot's bootstrapping methods. Panel **c** highlights our observed experiment-to-experiment variation.

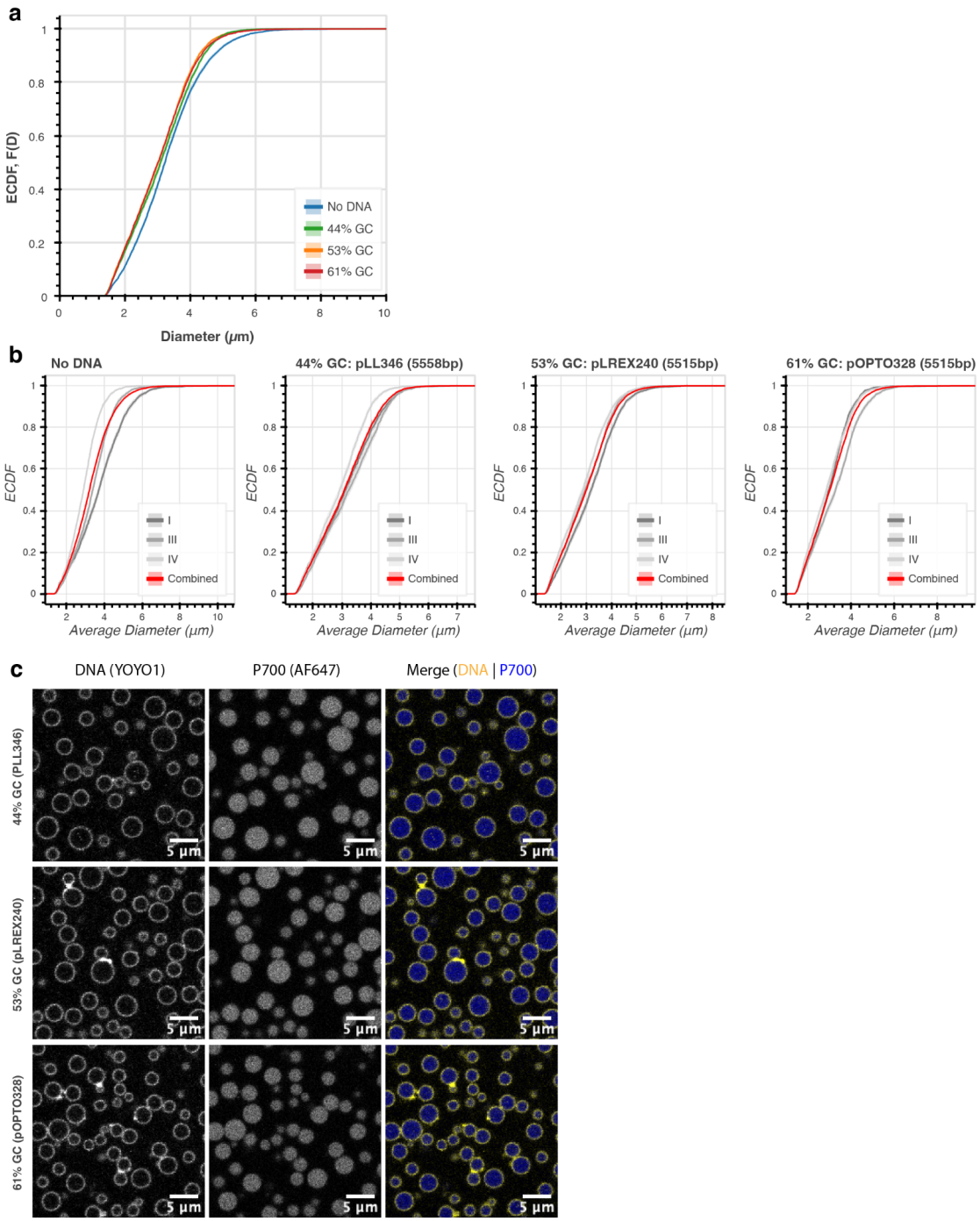

Supplementary Fig. 12. Varied GC content size quantification (No YOYO-1) & shell confirmation (with YOYO-1). a) The combined distribution ECDFs for plasmids of different GC content show similar distributions. Data is combined from three independent experiments as described our Methods section. b) ECDF curve for varied GC DNA showing distributions from individual experimental runs (grey) at 10 minutes with the combined distribution curve from **a** overlaid for reference (red). Shaded regions represent 95% confidence intervals calculated through Iqplot's bootstrapping methods. c) New samples imaged on confocal and in the presence of YOYO-1 to confirm the presence of shells for the plasmid sets used in the quantification experiments (scale bar = 5μm, n = 1).

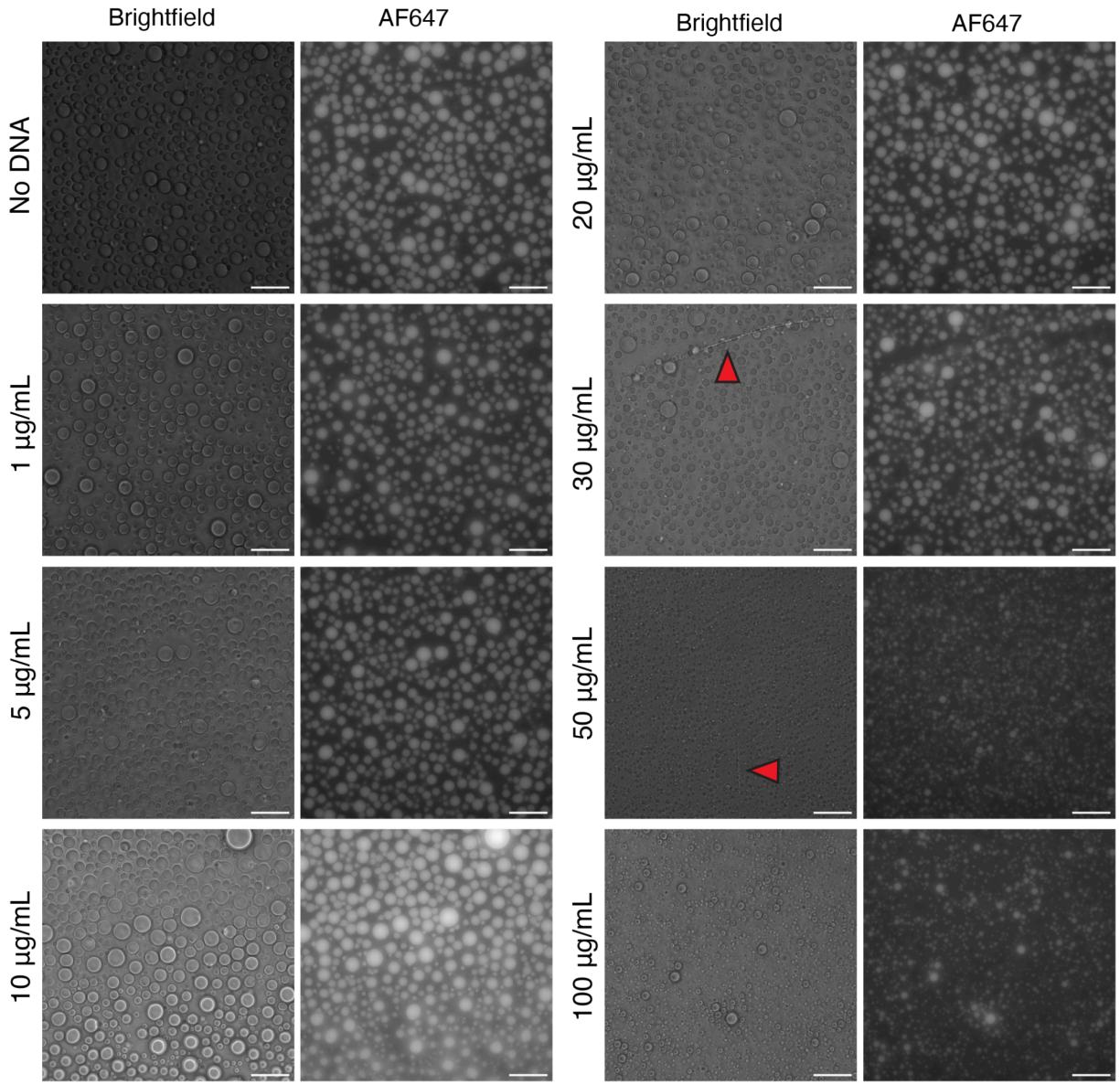

Supplementary Fig. 13. Representative widefield images in brightfield and fluorescence detection channels with varied DNA concentrations used for droplet size analysis (1mg/mL polyP, 100mM MgCl2, 50mM HEPES; scale bar = 20µm, n = 3). Filaments were observed in some fields of view above 30µg/mL DNA. Those visualized in these fields of view are indicated by red arrows. Each FoV shown is a cropped region from one of four FoV from a single experimental run used in the size quantification experiments (Fig 4b,c, & Supplementary Figs 16-17). For each size quantification experiment, three independent experiments were conducted as described in our Methods section.

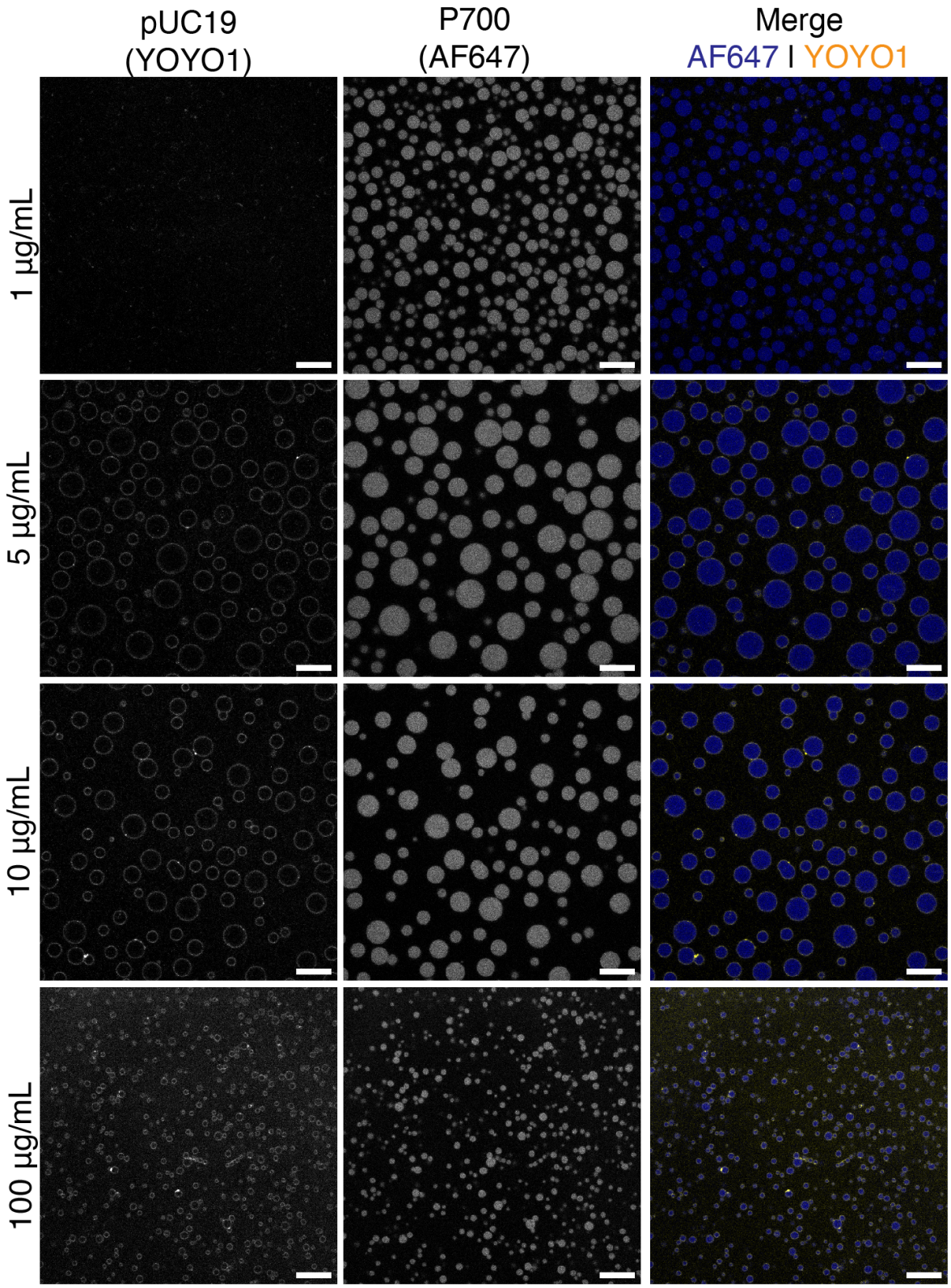

Supplementary Fig. 14. Representative confocal images of varied pUC19 concentration (1mg/mL polyP (10% P700-AF647), 100mM MgCl2, 50mM HEPES, 1µM YOYO-1; scale bar = 10µm, n = 1).

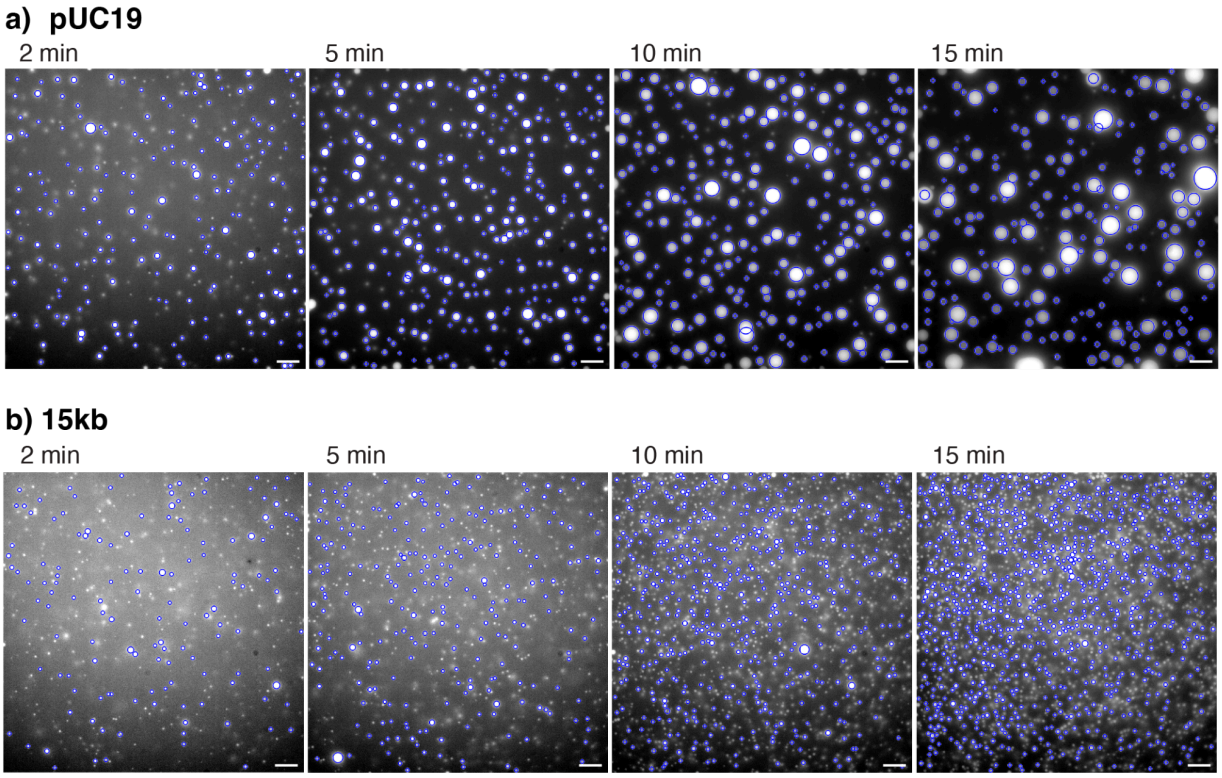

Supplementary Fig. 15. Representative overlays (blue) from segmentation step using the widefield 640 channel images for a) pUC19 and b) 15kb condensates. Images shown here were selected from the first of four fields of view from a single experiment at 2, 5, 10, and 15 min time points.

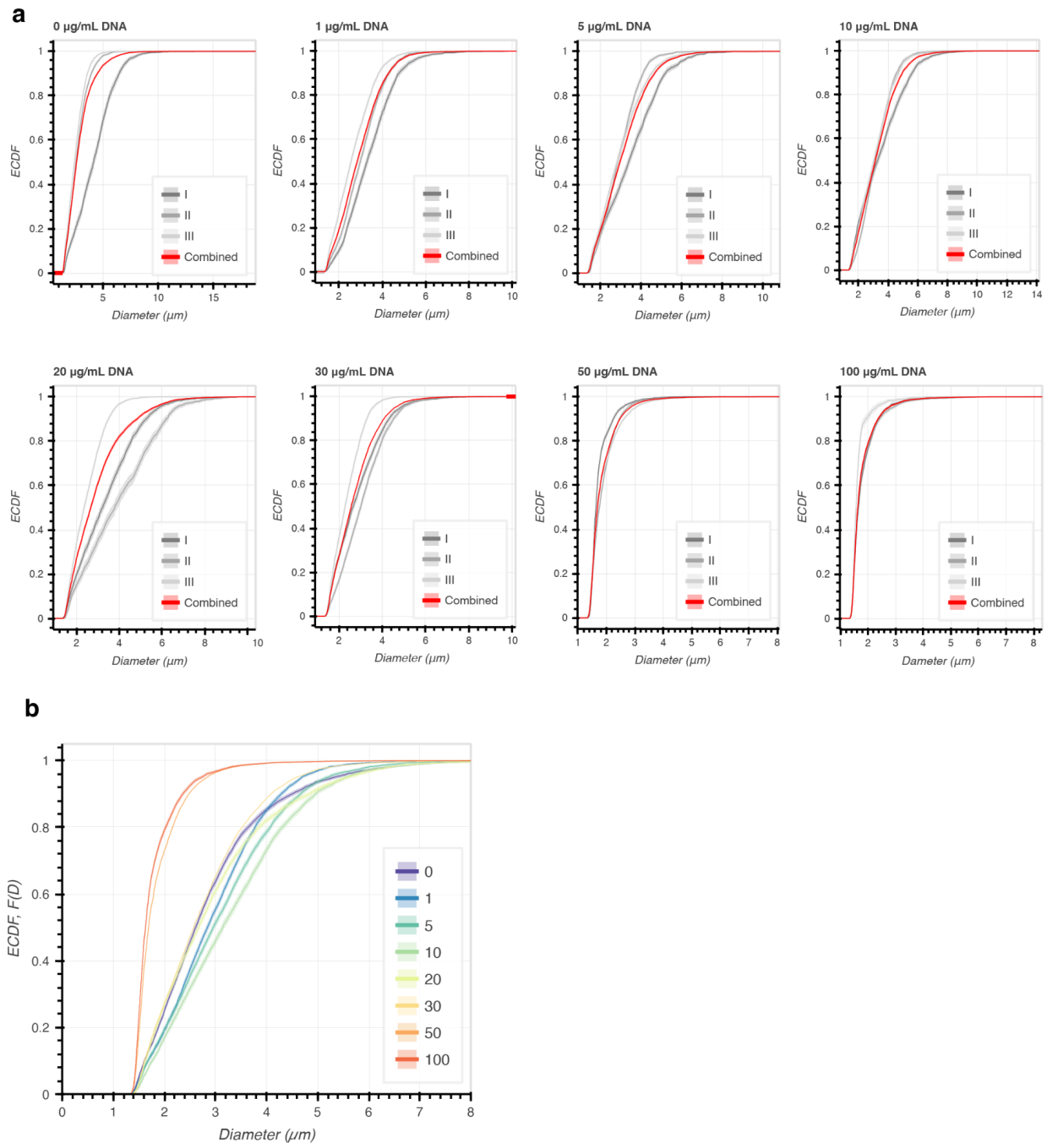

Supplementary Fig. 16. Experimental variation for DNA concentration experiments. a) ECDF curves showing cumulative distributions for varied DNA concentrations at 10 minutes for individual experiments (grey) and the combined distribution (red). Shaded regions behind the solid line represent 95% confidence intervals calculated through iqplot's bootstrapping methods. b) The combined distribution ECDFs shown in red in panel a are overlaid together for reference for the various DNA concentrations (n = 3).

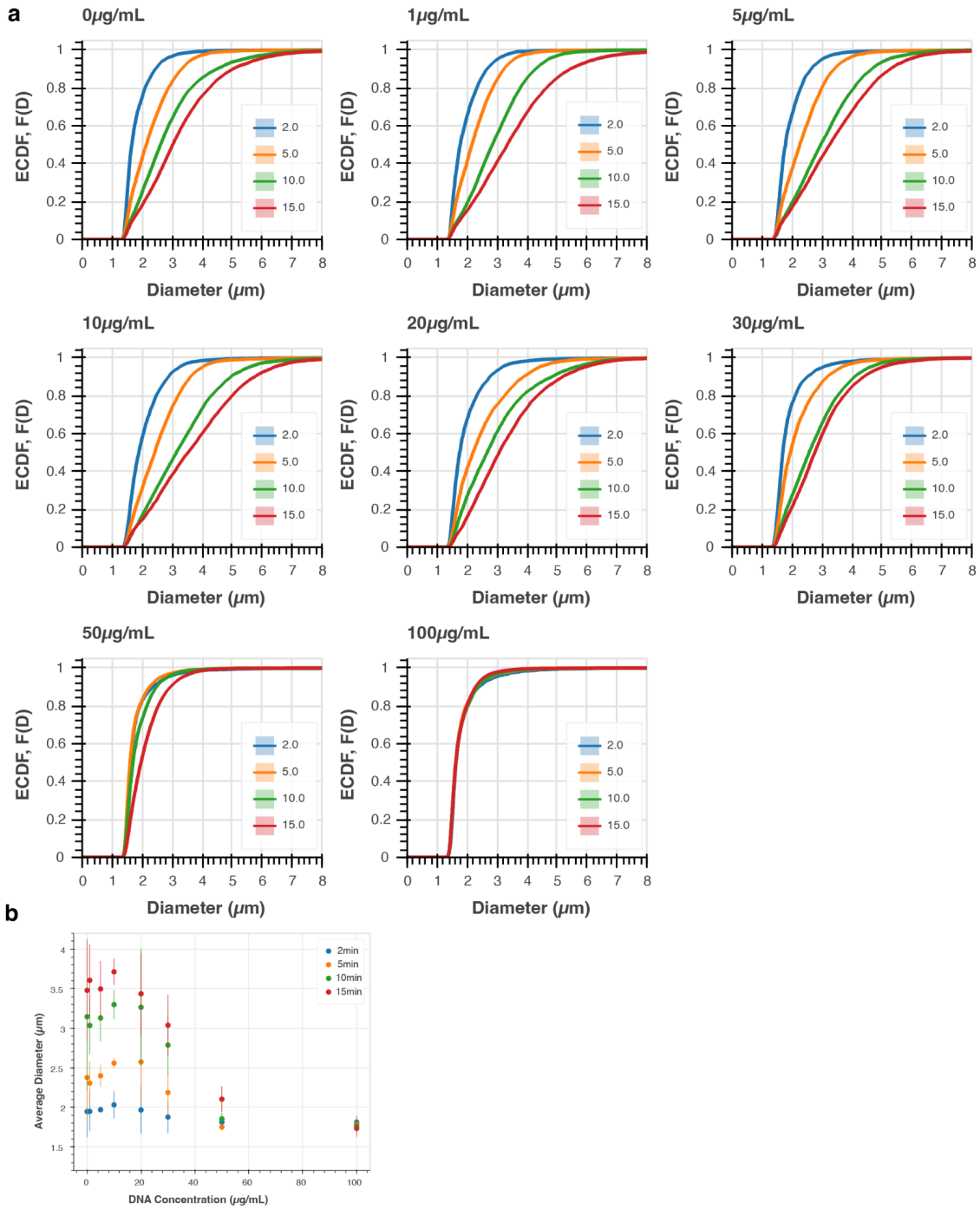

Supplementary Fig. 17. Time evolution of droplet size distributions for DNA concentration experiments. a) ECDF curves representing the cumulative distributions for varied DNA concentrations at 2, 5, 10, and 15 minute timepoints (n = 3). b) Compiled average of average diameters for various DNA concentrations at 2, 5, 10, and 15 minute time points across three experiments. Points represent the average of the mean diameter from individual experimental runs, while error bars represent the standard deviation from the mean of mean diameter for the three replicates.

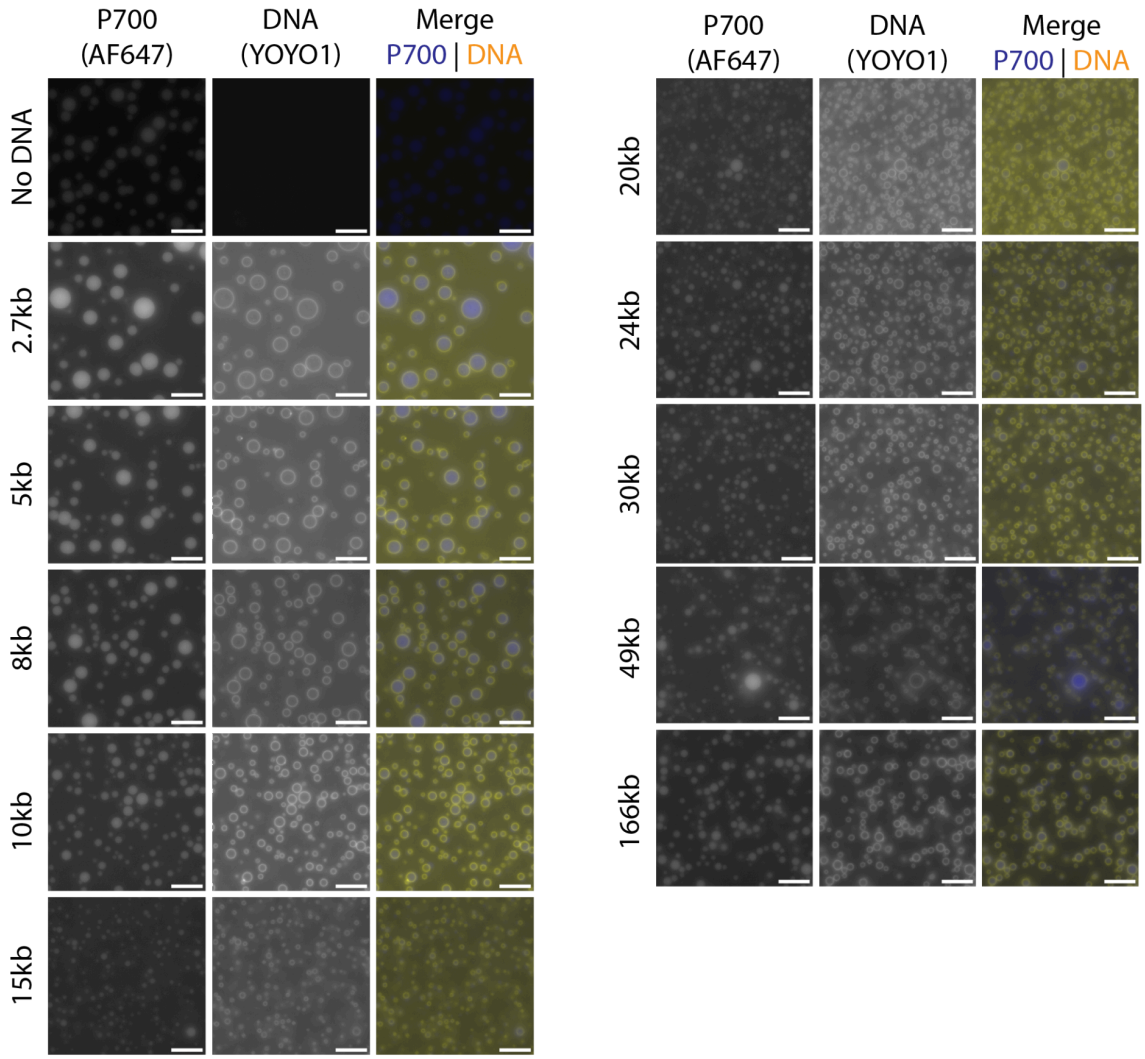

Supplementary Fig. 18. Representative widefield images with varied DNA lengths (1 mg/mL P700 (10% P700-AF647), 100mM MgCl2, 50mM HEPES,1 μM YOYO-1, 10ng/μL DNA; scale bar = 5μm). These are representative images selected from the size quantification experiment images (Figs 4d, e & Supplementary Figs 21-22). Individual channels are shown in gray, while the merge uses blue for polyP (P700-AF647) and yellow for DNA (YOYO-1). Each FoV shown is a cropped region from one of four FoV from a single experimental run. For each size quantification experiment, three independent experiments were conducted.

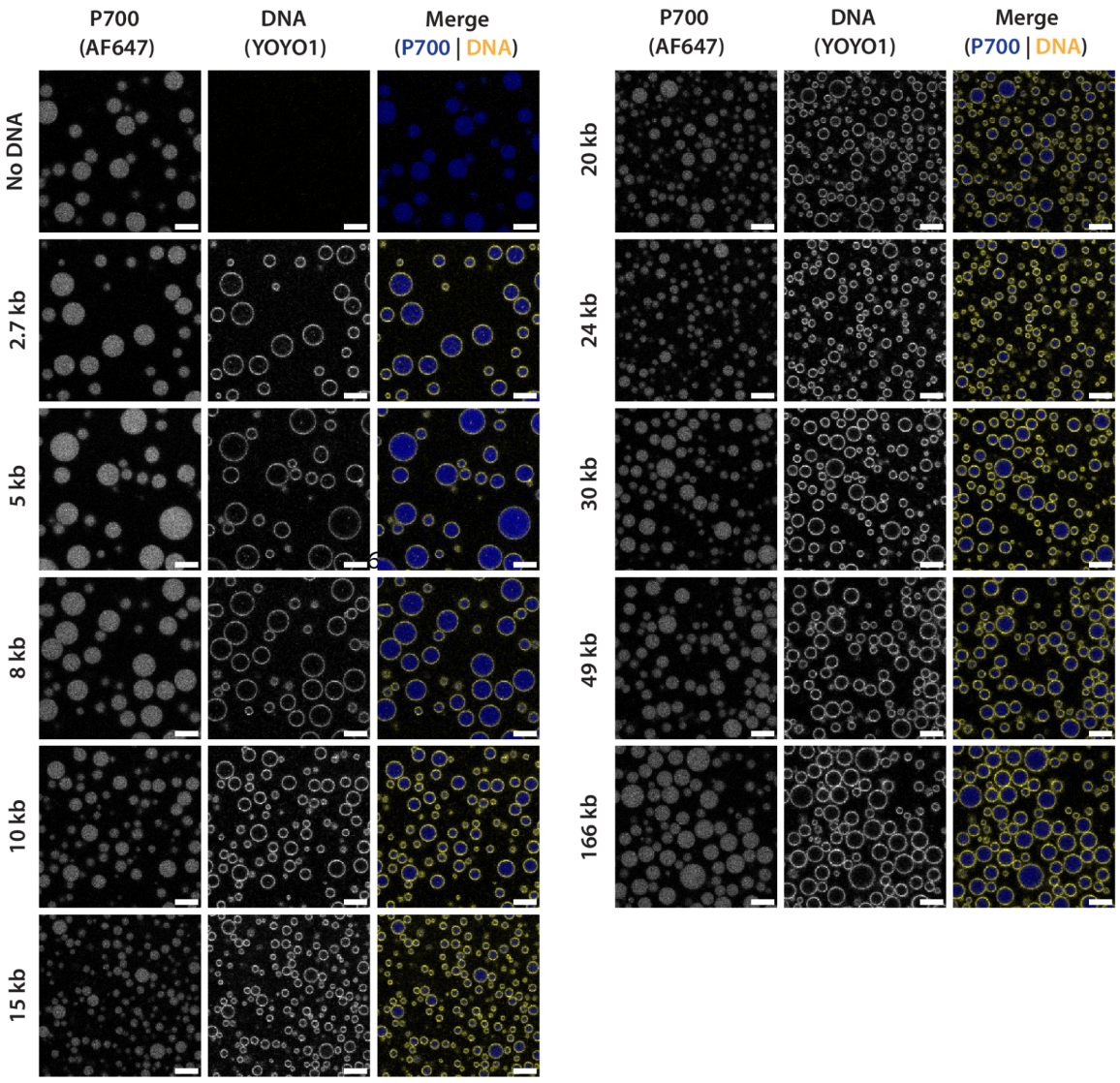

Supplementary Fig. 19. Representative confocal images with varied DNA lengths (1 mg/mL P700 (10% P700-AF647), 100mM MgCl2, 50mM HEPES,1 μM YOYO-1, 10ng/μL DNA; scale bar = 5μm, n = 1)

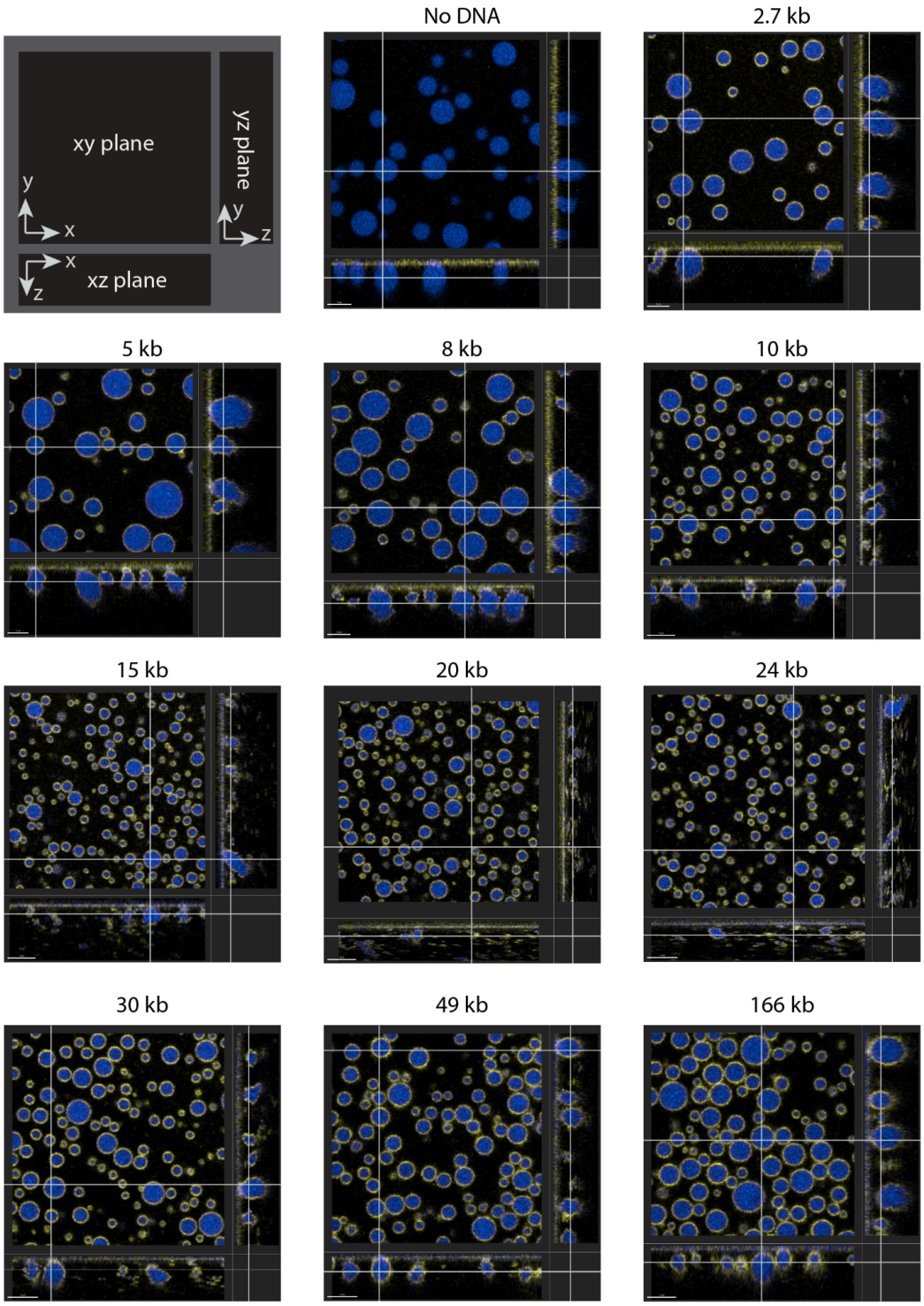

Supplementary Fig. 20. Imaris orthoview renderings of polyP-Mg^{2+}-DNA confocal z-stacks for varied DNA length experiments (1 mg/mL P700 (10% P700-AF647), 100mM MgCl2, 50mM HEPES,1 μM YOYO-1, 10ng/μL DNA; P700: blue, DNA: yellow; scale bar = 5μm, n = 1). Z-stacks were collected at 10 minutes after condensate formation with 0.37μm between frames, except for 20 & 24kb which were collected at 0.15μm and 30kb & 48kb which were at 0.30μm.

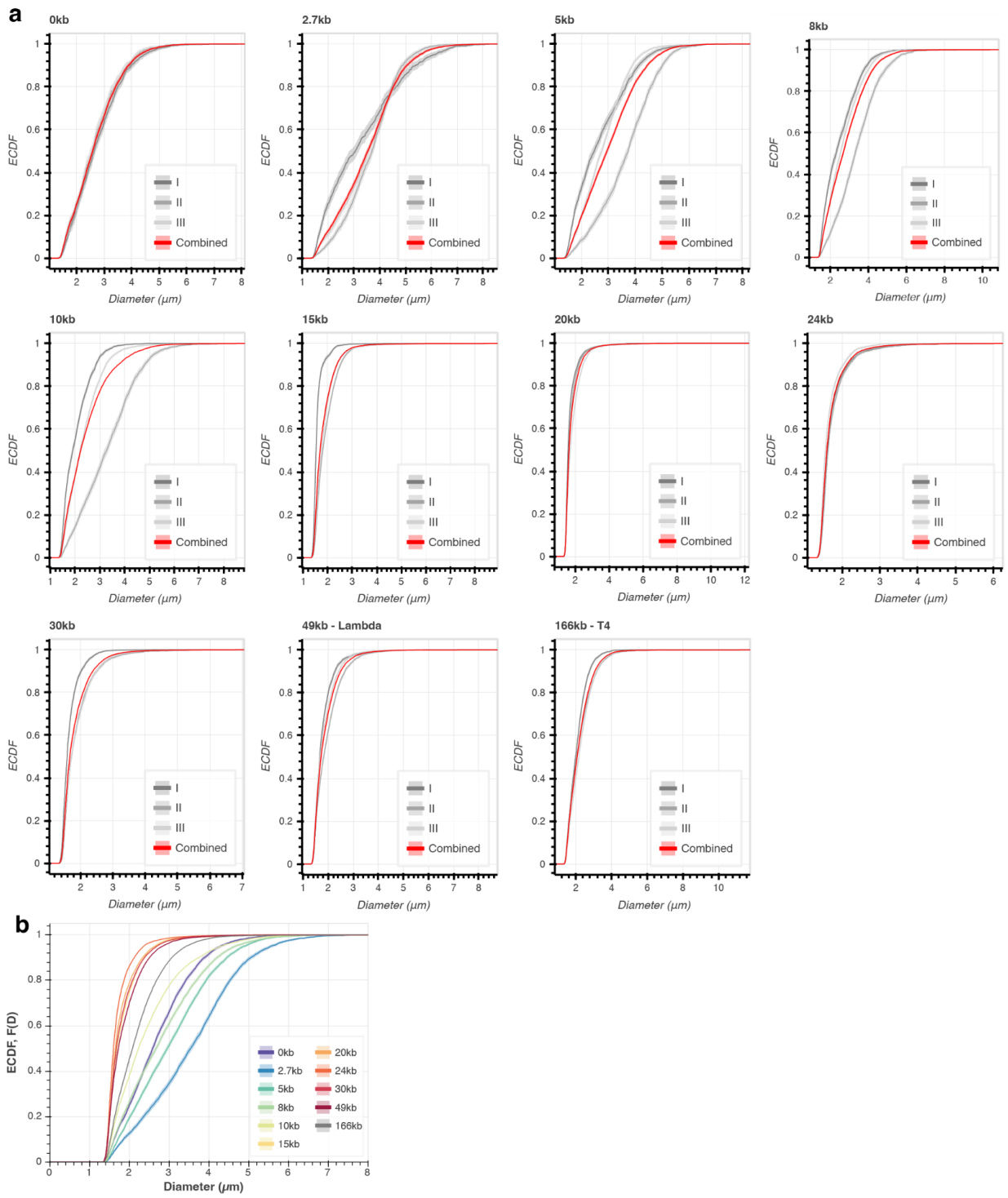

Supplementary Fig. 21. Experimental variation for DNA Length experiments. a) ECDF curves showing cumulative distributions for varied DNA lengths at 10 minutes for individual experiments (grey) and the combined distribution (red). Shaded regions behind the solid line represent 95% confidence intervals calculated through Iqplot's bootstrapping methods. b) The combined distribution ECDFs shown in red in panel **a** are overlaid together for reference for the various DNA lengths (n = 3).

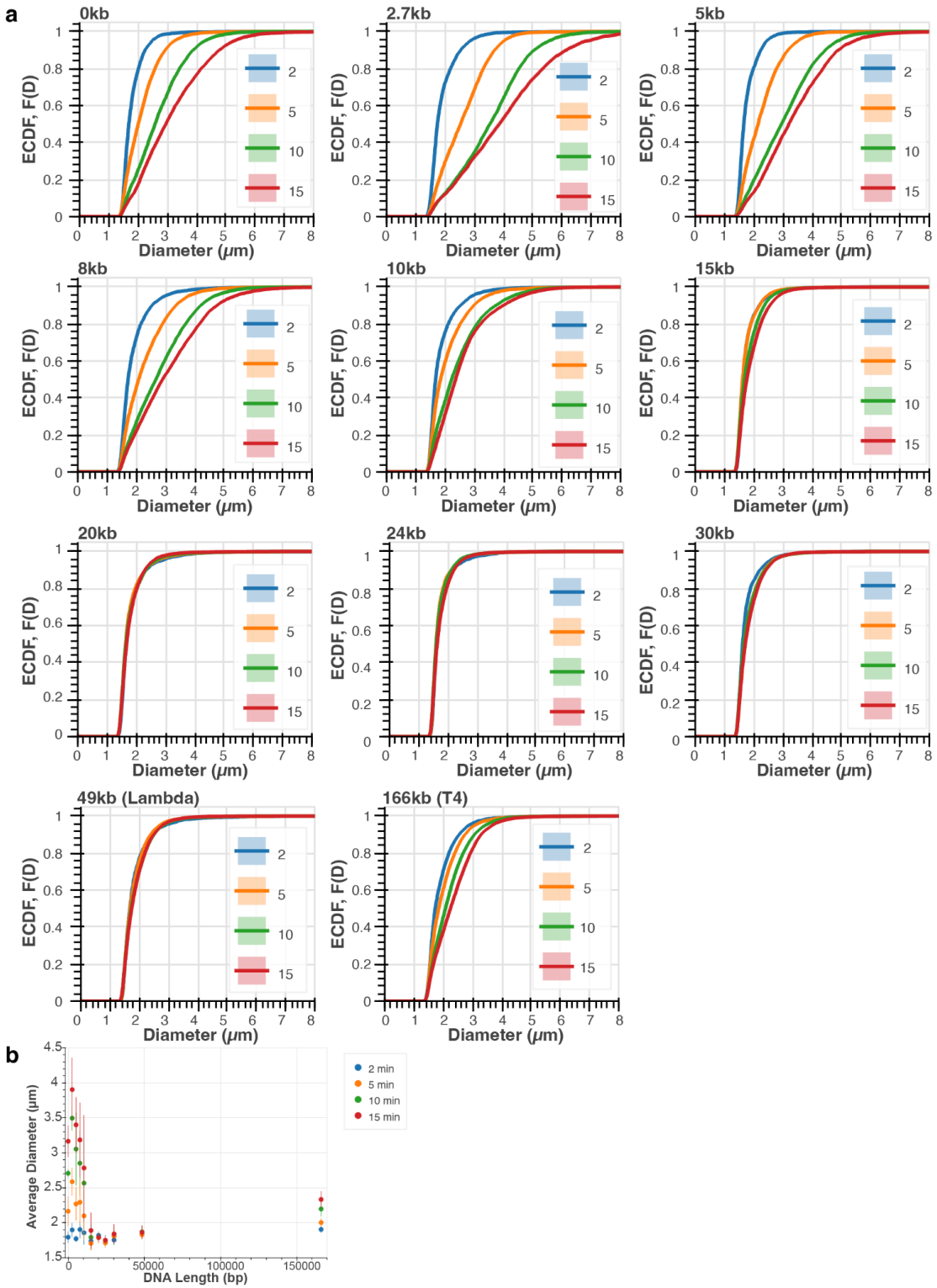

Supplementary Fig. 22.Time evolution of droplet size distribution for DNA Length experiments. a) ECDF curves representing the distributions with varied DNA length from compiled experiments (n = 3). b) Changes in the average droplet radii for DNA of different lengths are shown at 2, 5, 10, and 15 minutes after condensate formation. Points represent the average of the mean diameter from individual replicates (n = 3 replicates), while error bars represent the standard deviation of those mean diameters.

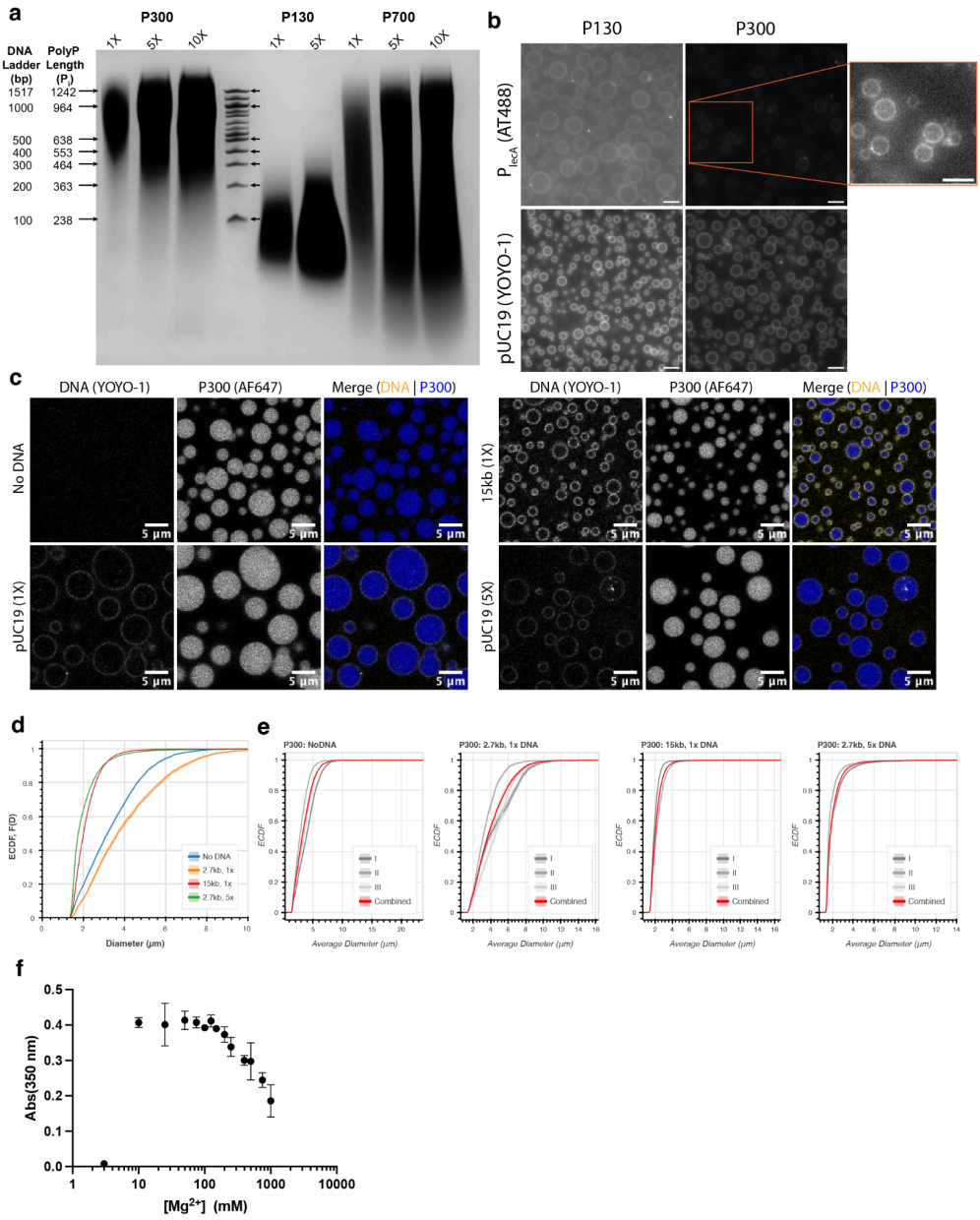

Supplementary Fig. 23. P130 & P300 shell formation and P300 size quantification. a) Commercial polyP samples P130, P300, and P700 have different size distributions based on polyacrylamide gel electrophoresis (n = 1) . 1X refers to 10 µg loaded in each lane (see Supplementary Methods). PolyP lengths correspond to DNA ladder bp lengths based on Smith et al. 2018[10]. b) Shells of ATTO488-P_{lecA} and pUC19 form at 100mM Mg^{2+} on P130 and P300-Mg^{2+} condensates ([polyP] = 1mg/mL, [Mg^{2+}] = 100mM, [DNA] = 10 ng/µL, [YOYO-1] with pUC19 only = 1µM, 50 mM HEPES pH 7.5, 10 min, scale bar = 10µm, n = 1). An inset with rescaled dynamic range is shown for P300 + P_{lecA}. c) DNA shells imaged with different DNA conditions using confocal microscopy ([YOYO-1] =1 µM, 10 min, n = 1). d) The combined distribution ECDFs for P300 with no DNA, 1X pUC19, 15kb, and 5X pUC19. ECDF curves showing cumulative distributions across three experiments for varied DNA conditions at 10 minutes (n=3). e) Individual experiments (grey) with the combined distribution curve used in **d** are overlaid for reference (red). Shaded regions behind the solid line represent 95% confidence intervals calculated through Iqplot's bootstrapping methods. f) Titration curve for P300 titration with Mg^{2+} quantifying absorbance at 350 nm ([P300] = 1mg/mL, 50mM HEPES pH 7.5, n = 4: 125mM, 250mM, 1000mM, n =3 for all others). Points and error bars represent the mean and standard deviation respectively of 3-4 replicates.

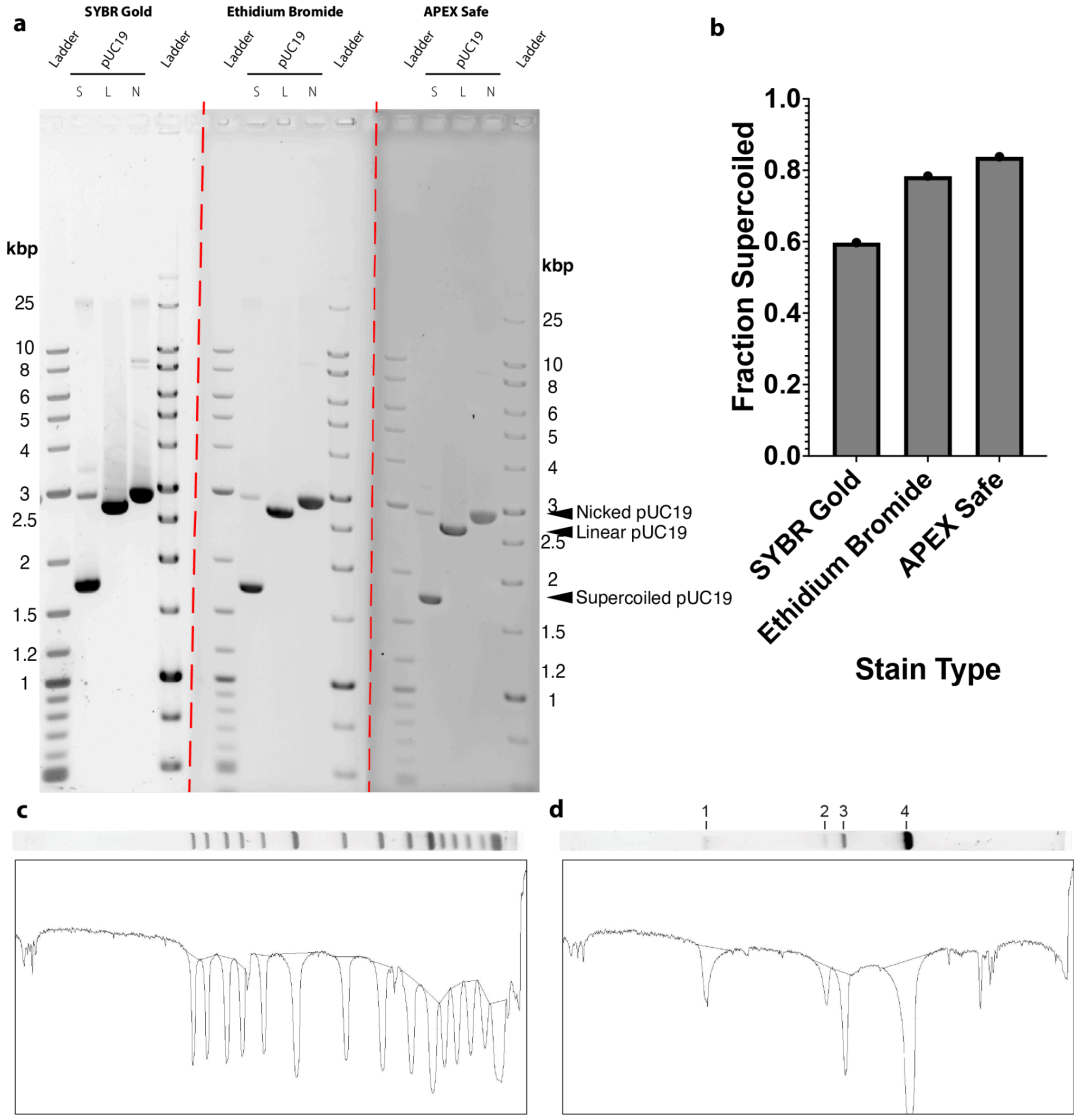

Supplementary Fig. 24. DNA quantification of pUC19 with different stains with representative band quantification traces. a) 200 ng of pUC19 samples ("S") with linearized ("L") and nicked ("N") controls for band identification. After electrophoresis, the gel was cut into three slices (indicated by dashed red line), and three different post-stains were used: SYBR Gold, Ethidium Bromide, and APEX™ Safe for comparison, with reference ladders and variations of pUC19 samples repeated for each set. Gels are shown next to one another for ease of visualization. b) Bands in the sample lane ("S") were quantified, and the fraction supercoiled was determined including all prominent bands, as described in the Supplementary Methods. c-d) Examples of quantification of supercoiled fraction of DNA samples. Gel quantification results of 1 kb plus ladder (c) and pUC19 (d) post-stained by SYBR Gold. A background subtraction was applied to better present the fluorescence intensity. The supercoiled fraction ratio was calculated as the ratio between fraction 4 to the sum of fraction 1-4. For all quantifications, n = 1.

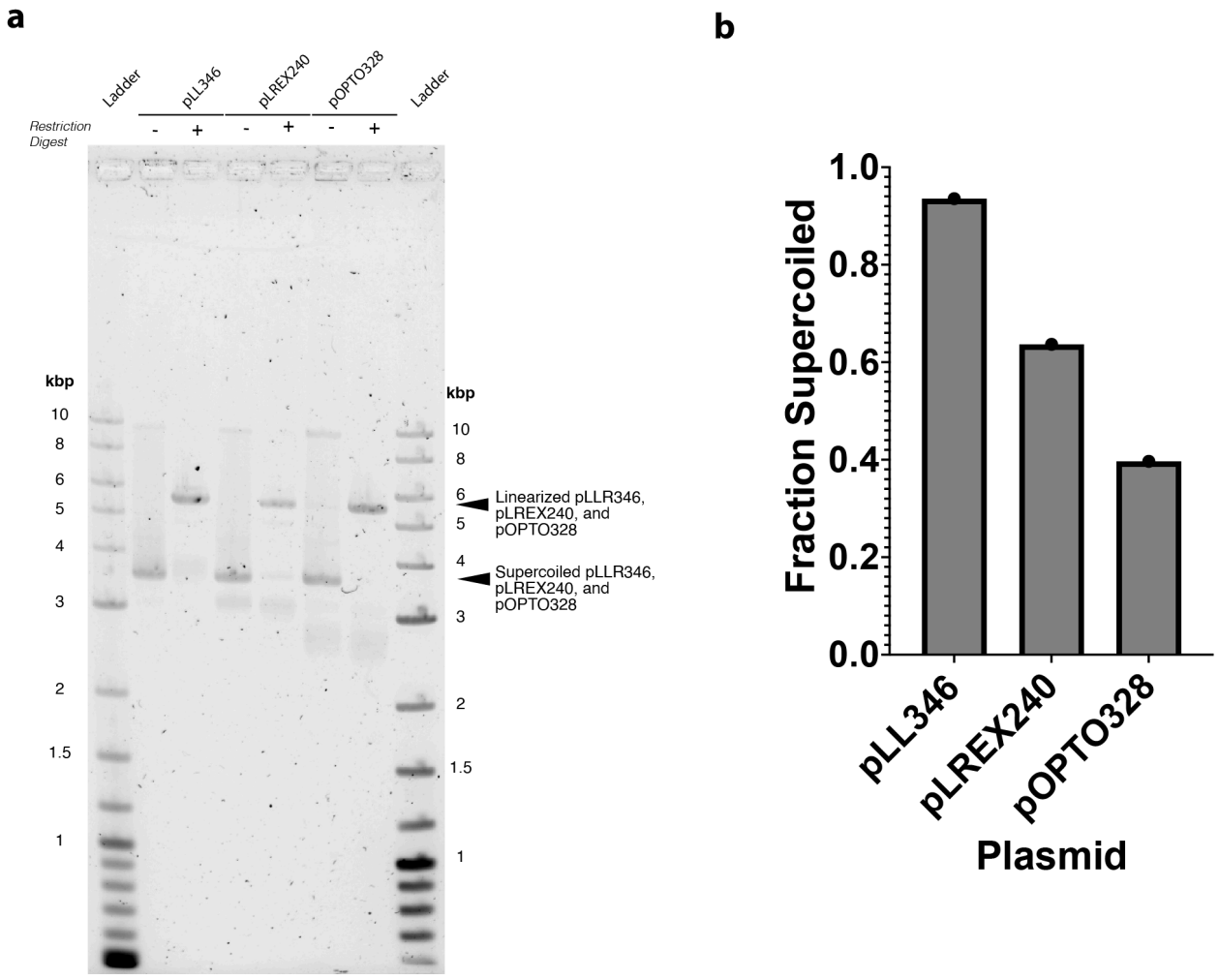

Supplementary Fig. 25. DNA quantification of plasmids used in GC content size quantification. a) 60 ng of DNA (+/- restriction digest) for each plasmid were loaded on 1% agarose gels and post-stained with SYBR Gold. b) Bands in the undigested lanes were quantified, and the fraction supercoiled was determined using the front most “supercoiled” band, and including all prominent bands, as described in the Supplementary Methods (n = 1).

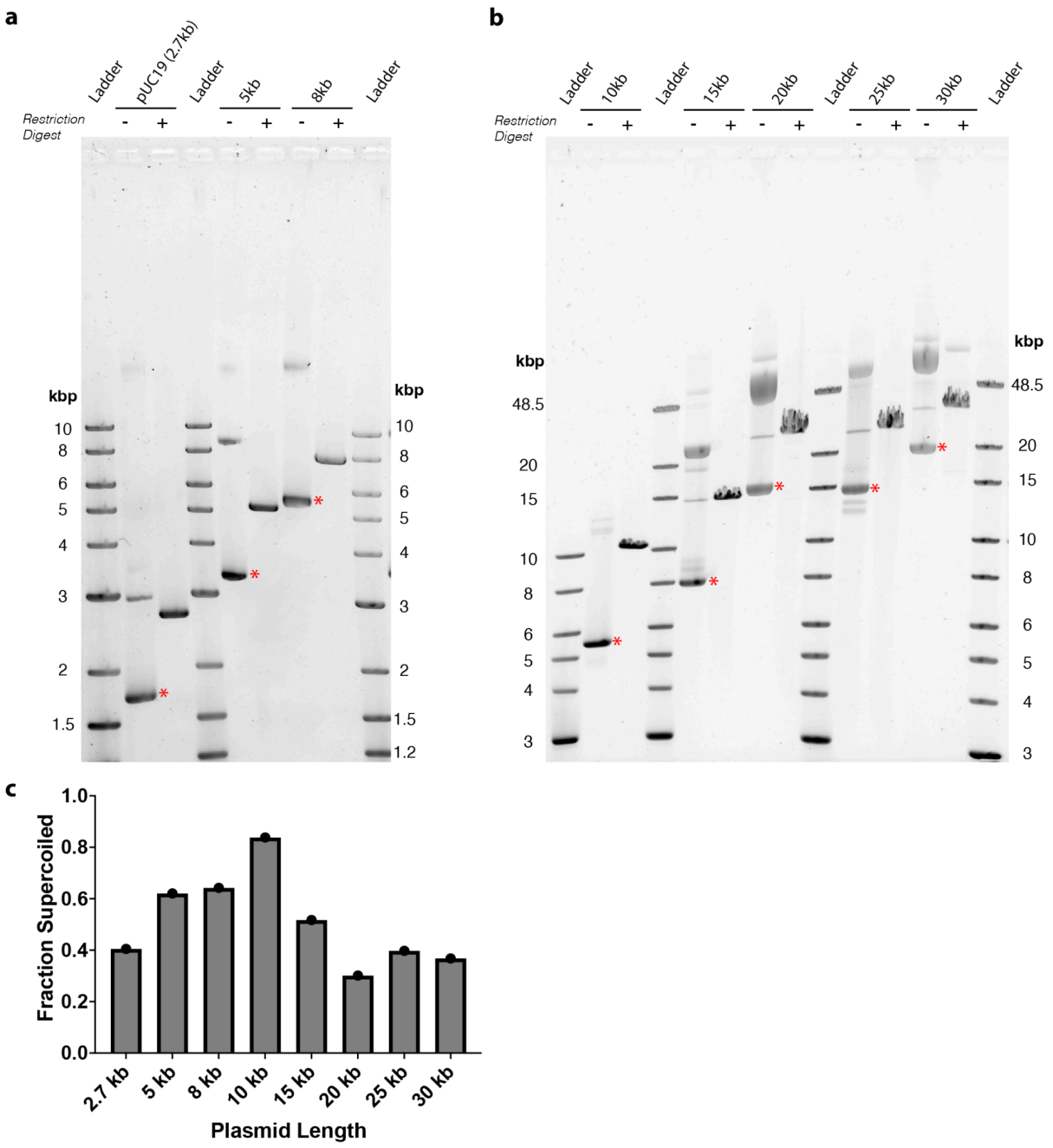

Supplementary Fig. 26. DNA quantification of plasmids used in DNA length experiments in absence of non-restriction digest based additives. 60 ng and 100 ng of DNA (+/- restriction digest) for each plasmid were run on (a) 1% agarose gel and (b) 0.5% agarose gel before SYBR Gold post-staining respectively. (c) Bands in the undigested lanes were quantified, and the fraction supercoiled was determined using the supercoiled bands (marked with the red star in **a** and **b**) and including all prominent bands, as described in the Supplementary Methods (n = 1).

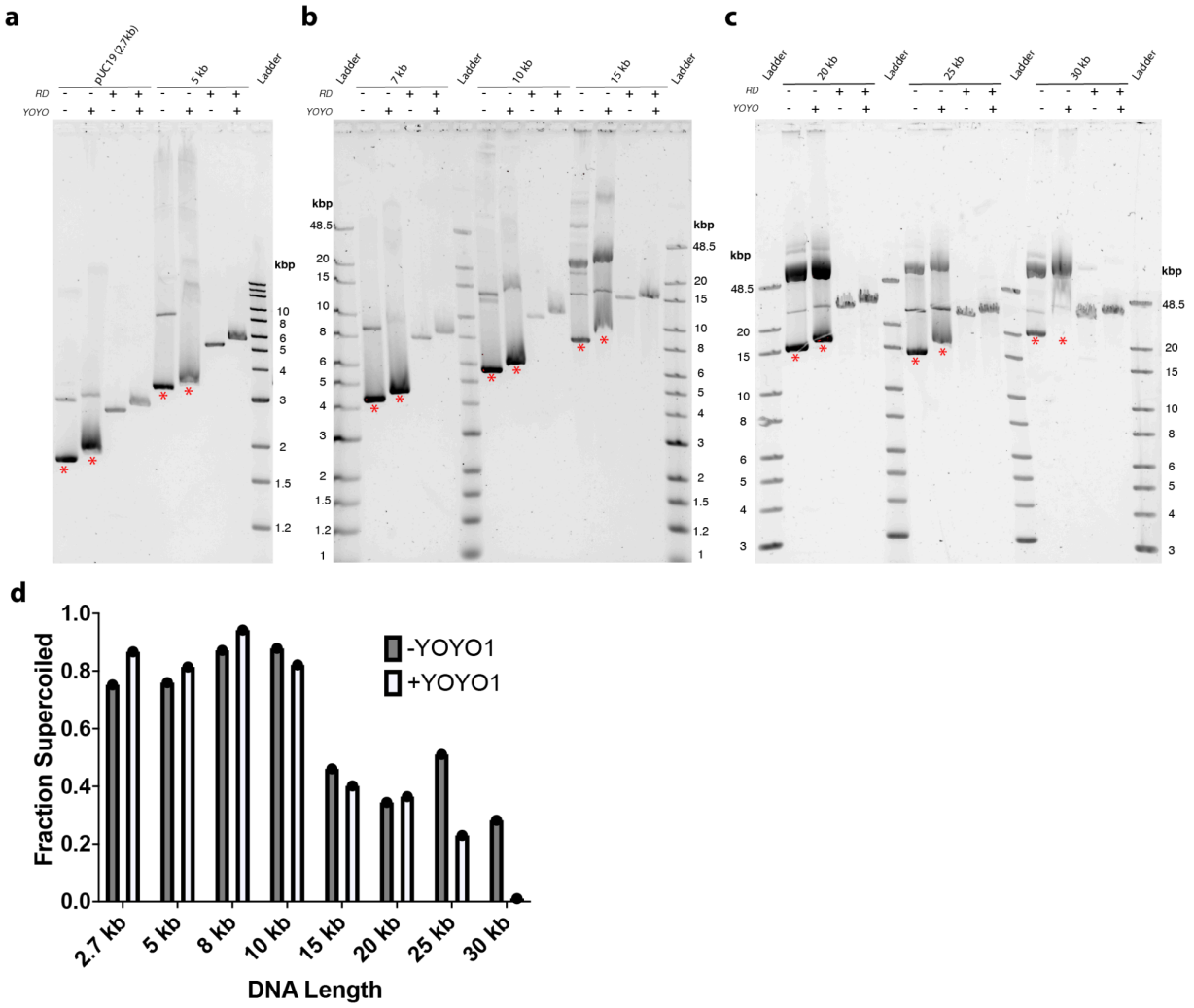

Supplementary Fig. 27. DNA quantification of plasmids used in DNA length experiments in 50mM HEPES and 100mM $MgCl_2$ +/- YOYO-1. 100 ng of DNA without YOYO-1 and 40 ng of DNA with YOYO-1 (+/- restriction digest, "RD") for each plasmid were resolved by agarose gel electrophoresis and stained after electrophoresis with SYBR Gold. Plasmids were grouped by length as follows: a) pUC19 and 5 kb (1% agarose), b) 7, 10, and 15 kb (0.5% agarose) and c) 20, 25, and 30 kb (0.5% agarose). d) Bands in the undigested lanes were quantified, and the fraction supercoiled was determined using the supercoiled bands (marked with the red star in **a**, **b, c**) and including all prominent bands, as described in the Supplementary Methods (n = 1).

REFERENCES

1. Kolbeck, P. J. *et al.* Molecular structure, DNA binding mode, photophysical properties and recommendations for use of SYBR Gold. *Nucleic Acids Res* **49**, 5143–5158 (2021).
2. Kolbeck, P. J. *et al.* Supercoiling-dependent DNA binding: quantitative modeling and applications to bulk and single-molecule experiments. *Nucleic Acids Res* **52**, 59–72 (2024).
3. Schindelin, J. *et al.* Fiji: an open-source platform for biological-image analysis. *Nat Methods* **9**, 676–682 (2012).
4. Green, M. R. & Sambrook, J. Isolation of High-Molecular-Weight DNA Using Organic Solvents. *Cold Spring Harb Protoc* **2017**, pdb.prot093450 (2017).
5. Meisner, J. & Goldberg, J. B. The *Escherichia coli* rhaSR-PrhaBAD Inducible Promoter System Allows Tightly Controlled Gene Expression over a Wide Range in *Pseudomonas aeruginosa*. *Applied and Environmental Microbiology* **82**, 6715–6727 (2016).
6. Shanks, R. M. Q., Caiazza, N. C., Hinsa, S. M., Toutain, C. M. & O'Toole, G. A. *Saccharomyces cerevisiae*-Based Molecular Tool Kit for Manipulation of Genes from Gram-Negative Bacteria. *Appl Environ Microbiol* **72**, 5027–5036 (2006).
7. Xu, P., Vansiri, A., Bhan, N. & Koffas, M. A. G. ePathBrick: a synthetic biology platform for engineering metabolic pathways in E. coli. *ACS Synth Biol* **1**, 256–266 (2012).
8. Baker, C. J., Smith, S. A. & Morrissey, J. H. Diversification of polyphosphate end-labeling via bridging molecules. *PLOS ONE* **15**, e0237849 (2020).
9. Choi, S. H. *et al.* Phosphoramidate End Labeling of Inorganic Polyphosphates: Facile Manipulation of Polyphosphate for Investigating and Modulating Its Biological Activities. *Biochemistry* **49**, 9935–9941 (2010).
10. Smith, S. A., Wang, Y. & Morrissey, J. H. DNA ladders can be used to size polyphosphate resolved by polyacrylamide gel electrophoresis. *Electrophoresis* **39**, 2454–2459 (2018).
11. Ghosh, A., Kota, D. & Zhou, H.-X. Shear relaxation governs fusion dynamics of

biomolecular condensates. *Nat Commun* **12**, 5995 (2021).

12. Alshareedah, I., Kaur, T. & Banerjee, P. R. Chapter Six - Methods for characterizing the material properties of biomolecular condensates. in *Methods in Enzymology* (ed. Keating, C. D.) vol. 646 143–183 (Academic Press, 2021).

13. Pappu, R. V., Cohen, S. R., Dar, F., Farag, M. & Kar, M. Phase Transitions of Associative Biomacromolecules. *Chem. Rev.* **123**, 8945–8987 (2023).